Chordotonal organs in hemipteran insects: unique peripheral structures but conserved central organization revealed by comparative neuroanatomy

Hiroshi Nishino*[1], Hiromi Mukai[2], and Takuma Takanashi[2]

[1]Research Institute for Electronic Science, Hokkaido University, Sapporo 060-0812, Japan, [2]Department of Forest Entomology, Forestry and Forest Products Research Institute, Matsuno-sato 1, Tsukuba, Ibaraki 305-8687, Japan

The number of text pages:

The corresponding author: Hiroshi Nishino, Research Institute for Electronic Science, Hokkaido University, Sapporo 060-0812, Japan.
Tel: +81-11-706-2596
Email: nishino@es.hokudai.ac.jp

Abbreviations: abCO: abdominal chordotonal organ; AEM: accessory extensor muscle; AN: auditory nerve; CG: central ganglion; CNS: central nervous system; CO: chordotonal organ; DET: distal extensor tendon; DL: dorsal ligament; DS: dorsal scoloparium; FCO: femoral chordotonal organ; F-T joint: femoro-tibial joint; JO: Johnston's organ; PG: prothoracic ganglion; PES: proximal extracellular space; PlCO: pleural CO; SC: scolopale cap; SEG: subesophageal ganglion; SGO: subgenual organ; SR: strand receptor; tyCO: tymbal CO; TeN: tensor nerve; TEPS: tibial extensor pendant sclerite; TyN: tymbal nerve; vCO: ventral CO; VL: ventral ligament; VS: ventral scoloparium; WGA: wheat germ agglutinin.

Keywords: insects; fat body cells; vibrational communication; central projection; proprioception

Running title: chordotonal organs in hemipteran insects

Abstract (within 250 words)

Hemipteran insects use sophisticated vibrational communications by striking body appendages to the substrate or by oscillating the abdominal tymbal. There has been, however, little investigation of sensory channels for processing vibrational signals. Using sensory nerve stainings and low invasive confocal analyses, we demonstrate the comprehensive neuronal mapping of putative vibration-responsive chordotonal organs (COs) in stink bugs (Pentatomidae and Cydinidae) and cicadas (Cicadidae). The femoral CO (FCO) in stink bugs consists of ventral and dorsal scoloparia, homologous to distal and proximal scoloparia in locusts, which are implicated in joint movement detection and vibration detection, respectively. The ligament of the dorsal scoloparium is distally attached to the accessory extensor muscle, whereas that of the ventral scoloparium is attached to a specialized tendon. Their afferents project to the dorso-lateral neuropil and the central region of the medial ventral association center (mVAC) in the ipsilateral neuromere, where presumed dorsal scoloparium afferents and subgenual organ afferents are largely intermingled. In contrast, FCOs in cicadas have decreased dorsal scoloparium neurons and lack projections to the mVAC. The tymbal CO of stink bugs contains four sensory neurons that are distally attached to fat body cells via a ligament. Their axons project intersegmentally to the dorsal region of mVACs in all neuromeres. Together with comparisons of COs in different insect groups, the results suggest that hemipteran COs have undergone structural modification for achieving faster signaling of resonating peripheral tissues. The conserved projection patterns of COs suggest functional importance of the FCO and subgenual organ for vibrational communications.

Introduction

Small animals such as plant dwellers often utilize vibration as a communication signal because vibration propagates a long distance through the substrate (Cocroft and Rodriguez 2005; Hill 2008). Heteroptera is one of animal groups that use vibrations extensively for various intraspecific communications such as mate attraction/rejection, courtship (Čokl and Virant-Doberlet 2003), and territorial aggression (Hayashi 1985). Moreover, low frequency vibrations are utilized by female shield bugs to promote egg hatching (Mukai et al. 2012, 2014) and to provision offspring (Nomakuchi et al. 2012).

The temporal pattern in a sequence of vibrations, called “songs”, are primary factors for conspecifics to evoke appropriate behavioral responses (Čokl et al. 2000; Miklas et al. 2001; McBrien and Millar 2003).

The diverse vibrational communications of stink bugs are assured by utilization of various body apparata. Substrate vibration is most commonly generated by percussion with the prothoracic legs (Zunic et al. 2008; Koczor and Čokl 2014), oscillation of the abdomen (Zunic et al. 2008; Kavcic and Čokl 2013), and quivering of the whole body (Numata et al. 1989). Moreover, similar to singing cicadas, vibration is also generated by muscle contraction of the tergal plate formed by fusion of abdominal tergites, called “tymbal” (review: Čokl 2008). The vibrations generated by popping the tymbal in and out are thought to be transmitted through the legs to the substrate (Zych et al. 2012).

Despite the diverse use of vibrations by stink bugs, the dominant frequencies of the vibrations generally lie in a narrow range, 100-150 Hz (review: Čokl 2008), being well tuned to the transmission properties of plants (Michelsen et al. 1982). Thus, the low attenuation of substrate vibrations enables long-range communication on the same plant under standing wave conditions (Čokl and Virant-Doberlet 2003), whereas airborne sound accompanied by vibration is strongly attenuated in the near-field range (Bennet-Clark 1998; Cocroft et al. 2000).

Although there have been extensive behavioral and spectral analyses of vibrational communications from phytophagous (Moraes et al. 2005) to predatory hemipteran insects (Laumann et al. 2013), little is known about sensory channels for processing vibrational signals. Ablation studies in shield bugs suggested the importance of leg sense organs for detection of substrate vibration emitted by conspecifics (Gogala et al. 1974). Neurophysiological recordings from sensory nerves in the southern green stink bug *Nezara viridula* indicated possible sense organs for detecting substrate vibrations (Čokl 1983; Čokl et al. 2006). Sense organs that are exquisitely sensitive to vibration and sound are internal stretch receptors ubiquitously found in body appendages of insects, called chordotonal organs (Field and Matheson 1998; Yack 2004). For example, the subgenual organ (SGO) located in the proximal tibia is the chordotonal organ specialized in detecting substrate vibrations (Lakes-Harlan and Strauß, 2014). The SGO in *N. viridula* contains only two sensory neurons (Michel et al. 1983), developing at a much lesser extent compared to that in orthopteran insects (Nishino and Field 2003; Strauß and Lakes-Harlan 2013). Electrophysiological recordings from leg nerves of *N.*

viridula indicated that one SGO neuron tunes to 200 Hz for the middle frequency and the other tunes to 700 ~1000 Hz, somewhat higher than the carrier frequency used for vibrational communications (Čokl 1983; Čokl et al. 2006). Thus, it has been proposed that joint chordotonal organs that generally tune to lower frequencies participate in detection of substrate vibrations emitted by conspecifics, in addition to their primary roles in proprioceptive mediation of the associated joints (Čokl and Virant-Doberet 2003).

The femoral chordotonal organ (FCO), which is conserved in almost all insect orders (Debeisieux 1935, 1938), is one of largest joint chordotonal organs (Field and Matheson 1998). The most distinctive structure of the FCO is the mechanical association of sensory neurons with a long chord-like cuticular apodeme extending from the proximal tibia (Field and Matheson 1998). Sensory neurons are therefore able to register indirectly tibial movement and position via apodemal movement and tension loaded on the apodeme, respectively. In orthopteran insects, sensory neurons in the FCO are functionally specialized for detecting various displacements of the apodeme from fast and small displacements, i.e., vibrations (Field and Pflüger 1989; Stein and Sauer, 1999) to slow and large displacements, i.e., joint movements (Field and Burrows 1982; Hofmann et al. 1985; Matheson 1990).

Chordotonal organs (COs) associated with the tymbal have been most extensively studied in cicadas, which primarily use sound for intraspecific communications (Young 1975, Young and Hill 1977; Simmons and Young 1978). Four COs (auditory CO, tymbal CO, tensor CO, and detensor CO) near the tymbal are among the most elaborate insect hearing organs, each having up to several hundred sensory neurons (Young 1975). In stink bugs, COs associated with the tymbal have not yet been identified.

Due to narrow-banded vibration emissions and frequent exchange duets between male and female (Čokl 2008), precise motor control of vibration production as an emitter as well as measurements of direction, intensity and frequencies of external vibrations as a receiver are needed for successful intraspecific communications by male and female stink bugs. Thus, one might speculate that stink bug COs undergo strong selective pressure to achieve quick and precise transduction of proprioceptive and vibrational signals.

So far, neuroanatomical study of COs in stink bugs has been limited to reconstruction from serial sections of legs in *N. viridula* (Michel et al. 1983). The

afferent morphology of individual COs is largely unknown. In order to gain insights into the early stage of vibrational processing in hemipteran insects, we selected the brown-winged green bug, *Plautia stali*, as a model insect due to amenability for dissections and subsequent observations of sense organs. Using selective and minute dye application into sensory neurons combined with immunostainings/counter stainings, we succeeded in the first comprehensive mapping of COs in body appendages with respect to those in other insect groups. The results demonstrated large modifications of CO structures, even between phylogenetically close hemipterans, in contrast to conserved central projections.

Materials and Methods

Animals

Three hemipteran species, two orthopteran species, and one coleopteran species were used, though most of the experiments were conducted in the brown-winged green bug, *Plautuia. stali*. Male and female adult *P. stali* (Pentatomidae) were cultured in the Forestry and Forest Products Research Institute. Shield bugs, *Parastrachia japonensis* (Cydnidae), were collected at a field site, Mt. Hinokuma, a small forested hill in Saga Prefecture, Japan (33º169N, 130º169E) in June 2015. Tympanate cicadas, *Lyristes bihamatus* (Cicadidae) and *Terpnosia nigricosta* (Cicadidae), were collected in Sapporo in August 2015 and May 2016, respectively. Migratory locusts, *Locusta migratoria*, collected in Saga Prefecture in October 2014, field crickets, *Gryllus bimaculatus*, cultured in Hokkaido University, and carabid beetles, *Zophobas atratus*, cultured in Kyusyu University, were also used. No sexual dimorphism was detectable in structures of COs and their central projections for all insects used in this study, also reported in previous studies (Young 1975; Michel et al. 1983; Jerum and Pabst 1996). Two hundred twenty *P. stali*, five *P. japonensis*, ten *L. bihamatus*, six *T. nigricosta*, eight *L. migratoria*, 20 *G. bimaculatus*, and 20 *Z. atratrus* were used for the experiments, though data presented are for smaller numbers of animals.

Retrograde and anterograde stainings of sensory neurons

After each animal had been cold-anesthetized, the whole body was fixed on a beeswax plate with the ventral side up by pinning in the lateral pronotum. The six legs

were laterally embedded in plastic wax. For retrograde labeling of CO sensory neurons, the peripheral nerves of interest were exposed and filled with Dulbecco's phosphate buffered saline (DPBS; D5773, Sigma Aldrich). The nerve was cut with microscissors (Vananas Scissors, 501778, WPI, FL, USA) and the distal cut-end was picked up by an electrolitically tapered tungsten rod (ID: 200 μm) with the tip slightly bent and placed in the tip of a tapered glass electrode filled with the microruby (dextran, tetramethylrhodamine and biotin, 3000 MW, ThermoFisher Scientific) (Fig. S1a) or 0.25 M nickel-cobalt mixture ($NiCl_2$:$CoCl_2$ = 22:3).

For anterograde labeling of axon terminals in the central nervous system (CNS), the peripheral nerve of interest was cut and its proximal cut-end was placed in the tip of a tapered glass electrode filled with the microruby (Fig. S1c), the microemerald (dextran, fluorescein and biotin, 3000 MW, ThermoFisher Scientific) or 0.25 M nickel-cobalt mixture. Care was taken not to stretch the nerve when handling. The preparation was left in a humidified chamber at 5 °C for 48 to 72 hours. The heavy metal-infused specimens were reacted with rubeanic acid in DPBS for 20 minutes (Fig. S1b, d) and processed for subsequent silver intensification (Bacon and Altman 1977). In fluorescent-dye infused specimens, the femur was left intact in *P. stali* because the covering cuticle is thin and translucent (Fig. S1a), while the anterior cuticle was removed to permit confocal observations in other insects. After fixation by 4% paraformaldehyde in PBS for 3 h at 5 ˚C, the specimen was dehydrated in an ethanol series and cleared in methyl salicylate.

Counterstaining and immunolabeling

In order to visualize the anatomical link between the FCO and surrounding structures such as muscles, we used two kinds of counterstaining with fluorescent dyes. For differential staining, the specimens in which nerves had been labeled with microruby were immersed in 0.5% Lucifer Yellow CH (Sigma Aldrich) in PBS for 40 min after fixation. To stain surrounding structures more permeably and intensely, the fixed specimens were immersed in 2% eosin dissolved in 95% ethanol before transferring them to 100% ethanol for 15 min in the dehydration process. The fat body cells were stained with 1% toluidine blue solution. To visualize F-actin filaments, the fixed specimens were transferred to 2.5% phalloidin solution (Acti-stain™ 488 Fluorescent Phalloidin, Cytoskeleton, Inc) for 1 h at room temperature before dehydration (Wolfrum,

1990). To stain N-acetyl-glucosamine (chitin), the fixed specimens were transferred to 1% wheat germ agglutinin solution (WGA, Alexa Fluor 488 Conjugate, ThermoFisher Scientific) for 30 min at room temperature before dehydration.

Microscopic observation of fixed specimens and data processing

The cleared specimens injected with fluorescent dyes and those injected with heavy metals were observed under a confocal laser scanning microscope (LSM 5 Pascal, Zeiss) and a light microscope (Imager Z1, Zeiss).

Specimens differentially labeled with microruby and Lucifer yellow (microemerald or Alexa Fluor 488) were visualized with an argon laser with a 505–530 nm bandpass filter and a helium-neon laser with a longpass filter (>560 nm), respectively. Specimens labeled with eosin were visualized with a longpass filter (>560 nm). Silver-intensified specimens were observed under the confocal microscope using reflection due to HeNe laser emission (HFT 543) combined with differential interference contrast. Thereafter, photomicrographs were taken by changing focus with a CCD camera (AxioCam MRc5, Zeiss) attached to the light microscope.

Optical sections were made at a resolution of 1024 x 1024 with 0.5-1.2-μm intervals throughout the entire depth of the legs and the CNS. Plan-Apochromat x10 0.8-NA and x20 0.8-NA (dry objectives) were used for observation of the legs and the CNS, and Plan-Neofluar x40 1.3-NA (oil immersion objective) was used for observation of sensory afferents and axon terminals. Observations were firstly made on wholemount preparations. Then, transverse sections of the CNS at 100~200 μm in thicknesses were made manually by using a twin bladed razor (0.1 mm in thickness, Feather, Japan) after the specimens had been rehydrated in 90 % ethanol.

The optical sections were converted to TIFF-formatted files using the software LSM Image Browser (Carl Zeiss, Jena, Germany). TIFF images were processed with image processing software (Amira ver. 3.1, Visage imaging, Berlin, Germany). The sensory neurons and surrounding structures were manually outlined in each optical section for subsequent three-dimensional representations using a volume rendering function. Three-dimensional surface models of internal structures of legs were obtained by surface rendering.

All photographic images were processed using Adobe PhotoShop Elements 6 (San Jose, CA). In figures, two to twenty consecutive photographs at different focal planes

were overlaid as aligned stacks and flattened to one plane.

Mapping of FCO neurons in intact legs

The unfixed leg of *P. stali* in which FCO neurons were retrogradely labeled (see above) was removed at the trochanter and embedded in a small portion of plastic wax in a hand-crafted glass chamber (1 mm in depth). Immediately after the tibia had been fixed at the fully flexed position (10˚), mid position (80˚), or fully extended position (150˚), the chamber was immersed in PBS with a thin cover slip of 0.04-0.06 mm in thickness (No. 000, Matsunami, Japan) and then observed under the LSM 5 Pascal. Both low-magnified and high-magnified optical images ware taken by using Plan-Apochromat x10 0.8-NA and Plan-Neofluar x40 1.3-NA, respectively.

Sensory neurons identified in optical sections were manually drawn by putting tracing paper on a monitor. The two-dimensional locations of sensory neurons were mapped on XY coordinates to the attachment site of the dorsal scoloparium as the fixed point (0). Statistical analyses (one-way ANOVA with Tukey's pairwise comparison) were subsequently conducted using R ver. 2.9 (R Development CoreTeam, 2009) to evaluate the distances of sensory neurons from the fixed point among the three tibial positions.

Terminology

We referred to Field and Matheson (1998) and Simmons and Young (1978) for the naming and terminology of chordotonal organs, to Michel et al. (1983) for grouping of FCO neurons, to Zorović et al. (2008) for the naming of ganglia, to Pflüger et al. (1988) for neuropils and tracts in the CNS, and to Furth and Suzuki (1990) for terminology of muscle tendons. The medial ventral association center (mVAC) that receives projections of COs is the concentric neuropil located between the ventral intermediate tract and the ventral medial tract in all thoracic neuromeres (Pflüger, 1988), and the mVAC is readily identifiable in hemipteran insects. The orientations of the COs and the CNS are shown in bodyaxis. The number of sample sizes is shown in parentheses in Results.

Results

Topographic structures of FCO and SGO in stink bugs

The peripheral nerve innervation pattern is well conserved in all six legs of the two stink bug species *P. stali* (Fig. 1a, b) and *P. japonensis* (Figs 1g and S1b). The FCO and SGO in each leg are innervated by a sensory nerve branch diverging dorsally at half of the femur from the main leg nerve (MLN, Fig. S1b). The sensory nerve travels antero-dorsally to innervate the FCO scoloparia located in the distal third of the femur (Figs. 1a-c and S1b). A thin nerve tributary diverging from the ventral region of the FCO scoloparia (inset in Fig. 1e, f) runs in parallel to the ventral ligament and innervates the SGO and exteroceptors (hair sensilla and campaniform sensilla) located in the proximo-dorsal region of the tibia (Fig. 1l-n).

Three-dimensional reconstructions of FCO neurons labeled with microruby (magenta) and surrounding structures counterstained with Lucifer Yellow (green) in *P. stali* revealed that the FCO scoloparia are firmly suspended to the antero-dorsal region of the cuticle (arrows, Fig. 1c, e). A thin membrane-like septum originates from the anterior cuticle just beneath the ventral region of the scoloparia (Figs. 1c and S4) and joins postero-distally in the thick, flattened tendon where the main extensor tibiae muscle fibers are obliquely attached (Fig. 1a). The FCO scoloparia and ligaments (except tips) are therefore separated from nearby muscle fibers (Fig. S4).

The FCO consists of two partly-fused scoloparia, the ventral scoloparium (VS) and the dorsal scoloparium (DS), which are distally connected to the ventral ligament (VL) and the dorsal ligament (DL), respectively (Figs. 1h, i and S4). The two FCO ligaments are composed of elongated attachment cells, as in those of lacewing FCOs (Lipovsek et al. 1999) and those of cicada tymbal COs (Young 1975). Chitin material (1 μm in thickness), stained by WGA, envelopes each ligament, conferring stiffness to the ligament (Fig. 1d). The ventral ligament runs in the anterior side of the femur (Fig. 1f) and it's distal tip ramifies into fan-shaped fibers, each attaching to different points of the dorsal region of the specialized extensor apodeme (Fig. 2a, b), termed the "tibial extensor pendant sclerite (TEPS)" by Furth and Suzuki (1990). The dorsal ligament is oriented posteriorly (Fig. 1f), and its distal tip swells and attaches to the postero-central region of the accessory extensor muscle (AEM) that bridges between the tip of the TEPS and the postero-dorsal cuticle (Fig. 2a, b). The lengths of the two ligaments in *P. stali* and *P. japonensis* are approximately 600 μm and 900 μm, respectively (Figs. 1a and S1b).

In ventral and dorsal scoloparia, two sensory neurons are paired and extend dendrites

into a common scolopale cap (SC, Fig. 1j, k), forming a single "scolopidium" (Field and Matheson 1998; Lakes-Harlan and Strauß 2014). Twelve scolopidia were stained in the FCO in *P. stali*, the same number as that for *P. japonensis* (Table 1) and for *N. viridula* (Michel et al. 1983). Five pairs of neurons are arranged in the proximal region of the ventral scoloparium, while four additional pairs of distal neurons (d1-d4, Fig. 1e, g) are embedded in connective tissues that are attached to the side of the ventral ligament (Fig. 1e, g; Table 1). The dispersed and progressively smaller soma arrangements in the ventral scoloparium resemble those in the distal scoloparium of the locust (Matheson and Field 1990) and those in the ventral scoloparium of the cricket (Nowel et al. 1995). On the other hand, three pairs of sensory neurons in the dorsal scoloparium are proximo-posteriorly clustered closely to the attachment site of the dorsal cuticle (Fig. 1h), resembling the clustering manner of proximal scoloparium neurons in the locust (Field and Pflüger 1989) and dorsal scoloparium neurons in the cricket (Nishino 2000) and the weta (Nishino 2003).

The morphology of the SGO in *P. stali* is similar to that in *N. viridula* (Michel et al. 1983) in that it holds two scolopidia each with one sensory neuron (yellow arrows, Fig. 1l-n). These sensory neurons extend dendrites to different sites of a common ligament that distally attaches to the dorso-distal tibia (Fig. 1n; Michel et al. 1983). The hemolymph channel is proximally clogged by a bundle of specialized muscle fibers diverging from the retractor unguis that bridges between the dorsal hypodermis and the longitudinal muscle (white arrows, Fig. 1l, m).

Structure of attachment sites of FCO ligaments in stink bugs

Next, we investigated the structure and movement of the TEPS and AEM, to which the ventral and dorsal ligaments of the FCO are attached, as these structures are crucial for conferring distinct sensitivity to ventral and dorsal scoloparium neurons.

The TEPS is distally attached to the proximo-dorsal tibia via the distal extensor tendon (DET) that spans about 100 μm (Fig. 2c). Since the TEPS is highly sclerotized (Furth and Suzuki 1990), the angles made by the TEPS and the tendon hardly change with tibial movements (Fig. 2c, d). Thus, axial movement of the ventral ligament is permitted, but its ventro-dorsal deflection is hampered by the TEPS. This situation differs from the movement of the cuticular apodeme in other insect FCOs, which rolls in distally with the tibial flexion and rolls out proximally with the tibial extension

(Shelton et al. 1992; Nowel et al. 1995).

The AEM attached to the tip of the hook-like TEPS (Fig. 2a-d) provides a high leverage to counter the intrinsic flexor tension by pulling the tip of the TEPS laterally against the proximo-distal movement of the main extensor tibiae muscle, so that extended tibial posture can be maintained by weak contraction of the AEM.

The AEM receives innervation of a dorsal branch diverging from the extensor nerve (marked by blue arrows in the inset of Fig. 2e). Therefore, the main extensor muscle and the AEM are very likely to be co-innervated by the slow extensor tibiae motoneuron, as in locusts (Evans and O'shea 1978). The innervation is confined to the proximal half (posterior cuticle side) of the AEM so that the attachment site of the dorsal scoloparium is free from motoneuronal innervation (Fig. 2e, f). Such a local motoneuronal innervation was the case for AEMs of pro, meso and metathoracic legs (n=3 for each).

Sensory neuronal displacements by passive femoro-tibial (F-T) joint movement in stink bugs

Since the leg cuticles of *P. stali* are thin and translucent and FCO scoloparia are located just beneath the anterior cuticle, nonfixed FCO neurons labeled with microruby could be visualized under a confocal microscope. Quantitative analyses of cellular movements when the tibia was held at 10˚ (full flexion), 80˚ (mid range) and 150˚ (full extension) in four mesothoracic legs revealed that the ventral scoloparium stretched distally with tibial flexion (Fig. 3a-c) and loosened proximally with tibial extension (Fig. 3a"-c"). The distally located neurons on the ventral ligament tend to be displaced at larger amounts than do proximally located neurons, being especially prominent in the extended range. The distances between distal neurons (d1 and d2c, Fig. 3a-c) and the fixed point of the scoloparia (0, Fig. 3a-c) are significantly smaller in full extension (Fig. 3a"-c") than in mid-position (Fig. 3a'-c') or in full flexion (Fig. 3a-c; one-way ANOVA with Tukey's pairwise comparison, Fig. 3d). The distances between paired neurons residing in the ventral scoloparium tend to be larger in the flexed range, as exemplified in d1 and d2 pairs (Fig. 3d). This suggests that tension is loaded both distally and proximally on the ventral scoloparium when the ligament is taut. In contrast, dorsal scoloparium neurons are hardly displaced in any tibial position due to their firm attachment to the dorsal cuticle (Fig. 3a, a', a", b, b', b", c, c', c"). We confirmed

similar cellular displacements in prothoracic FCOs (n=3) and metathoracic FCOs (n=4).

Structures of the FCO and SGO in cicada

The locations of pro-, meso- and metathoracic FCOs and their innervation patterns in cicadas are similar to those in stink bugs (FCO scoloparia indicated by yellow arrows, Fig. 4a, b). There are six pairs of neurons in the proximal region (Fig. 4c) and four pairs in the distal region of the ventral scoloparium (d1-d4, Fig. 4c). The counterpart corresponding to the dorsal scoloparium of stink bugs exists in cicadas but contains only two pairs of sensory neurons in *L. bihamatu*s and *T. nigricosta* (Fig. 4c, d). Otherwise, the composition of FCO neurons is similar to that of stink bugs in all legs (Table 1), although the first distal pair of neurons (d1) in the ventral scoloparium tend to be more closely located to the proximal neurons in cicadas (inset, Fig. 4c). The dorsal ligament that consists of two elongated attachment cells (Fig. 4e) runs in parallel with the ventral ligament and attaches to the joint pivot of the tibia where the extensor muscle apodeme is inserted. No specialized tendon like the TEPS is detectable in pro, meso, and metathoracic femora (Fig. 4a, b).

The thin nerve tributary diverging from the FCO scoloparia innervates two SGO scolopidia and several exteroceptors (hair sensilla and campaniform sensilla) in all tibiae of the cicadas *L. bihamatu*s (inset, Fig. 4c) and *T. nigricosta* (Fig. 4g). The locations of the SGOs in all tibiae were nearly identical to those in stink bugs. However, their distal structures differ in prothoracic and meso/metathoracic legs. In the prothoracic leg, the two sensory neurons extend dendrites to a long ligament that swells distally and attaches to the dorso-distal region of the femur (Fig. 4g), resembling the stink bug SGO in overall morphology. In the meso and metathotacic legs, two sensory neurons with two scolopale caps (inset, Fig. 4f) distally attach to a short ligament (Fig. 4f). The ligament swells like a horn and attaches to a septum located between the dorsal cuticle and the longitudinal trachea (Fig. 4f), resembling the structure of the lacewing SGO (Devetak and Pabst 1994).

Comparison of FCOs in different insect groups

Anterograde labeling of FCO neurons and subsequent F-actin-filament staining with phalloidin revealed distinct morphological features of two scoloparia, conserved across hemi- and holometabolous insects (Fig. 5). As phalloidin intensely stained scolopale

rods (Wolfrum 1990), elaborate dendritic segments that had been shown in low power TEM studies (Field and Matheson 1998; Wolfrum 1990) were detectable in high power confocal observations using an oil immersion objective.

Firstly, the connective tissues suspending the dorsal scoloparium to the proximal cuticle are rich in F-actin filaments, as exemplified in the cricket (white arrow, Fig. 5e) and the stink bug (white arrow, Fig. 5i). Likewise, F-actin filaments in the dorsal ligament (white arrows, Fig. 5a, b, d, k) are more than doubled compared to those in the ventral ligament (yellow arrows, Fig. 5a, b, d, k).

The morphology of the distal segment of dendrites also differs between the two scoloparial neurons. In ventral scoloparium neurons, the scolopale cap (SC, Fig. 5h, l) and adjoining distal extracellular space are thinner than the proximal extracellular space (PES, Fig. 5h), showing a "thin arrowhead-like shape" (Figs. 5h, j, l and S5). On the other hand, the scolopale cap and the distal extracellular space in dorsal scoloparium neurons are enlarged to be the same as or even larger than the proximal extracellular space, showing a "contour bottle-like shape" (Figs. 4d, 5g, j, m, and S5). The morphological features seen in the dorsal scoloparium neurons are shared by those of the stink bug SGO and cicada SGO (compare Fig. 5g with Fig. 1n and inset in Fig. 4f), proximal scoloparium neurons of locust FCOs (Moran et al. 1977), cricket tympanal CO (Fig. 5f), and cicada tymbal COs (Young 1975; Doolan and Young 1981).

In contrast to direct attachment of ligaments to the peripheral tissues in stink bugs and cicadas, two ligaments in other insects are distally merged into one and surround the coiled cuticular apodeme (cricket, Fig. 5n) or uncoiled apodemes (locust, Fig. 5o, p), which are invaginated from the endocuticle of the proximo-dorsal tibia.

Peripheral innervation and structure of the tymbal CO in stink bugs

The proximal four segments of the abdomen are innervated by the central ganglion (CG) in which meso, meta and abdominal neuromeres are fused (Zorović et al. 2008). Our preliminary experiments in *P. stali* showed that among four nerves located between the main leg nerve (MLN) and the descending connectives (DC) (Fig. S2a), a single nerve running just medial to the main metathoracic leg nerve (fourth nerve counting from the DC) is the "tymbal nerve (TyN)" that innervates exteroceptors, tymbal muscles and an associated CO, termed the tymbal CO. This nerve is locationally homologous to the tensor nerve in cicadas (Simmons and Young 1978) and the tympanal nerve in

locusts (Halax et al. 1988). Judging from central projections, each of the remaining three nerves (N1-3) contained one or two CO neurons, in addition to exteroceptor axons and motoneuronal axons (Fig. S2b-g).

The tymbal nerve descends along the ventral region of the metathorax and gives rise to a thick motor nerve that innervates two muscles (Fig. 6a, b). A thin tributary diverging from the motor nerve innervates the tymbal CO (Fig. 6a, b). Connective tissues containing four sensory neurons (Fig. 6c) are fixed to the ventral cuticular ridge between the metathorax and the abdominal sternites (indicated by yellow circles, Fig. 6f). The ligament is oriented dorso-laterally and terminates in the surface of fat body cells (Fig. 6d) that attach to the posterior surface of the tymbal muscle (Fig. 6b). The fat body cells, rich in lipids, are ubiquitously distributed in the body lumen (Figs. 6e and S1e-g). The length of the ligament is approximately 400 μm (Fig. 6d).

Abdominal chordotonal organs in stink bugs

The distal four abdominal segments are innervated by the descending connective (DC) from the central ganglion (Figs. 6f and S2a). There are two populations of COs. One group is located in the pleural fold between tergites and sternites of abdominal segments, designated pleural COs after Hustert (1978). Each pleural CO contains one sensory neuron (Fig. 6g, h). The cell body is attached proximally to the dorsal region of the spiracle muscle (reddish region indicated by blue arrows, Fig. 6f), while the dendrite is extended distally via a ligament at approximately 150 μm in length to the surface of fat body cells located just beneath the endocuticle (Fig. 6h). The location, number of sensory neurons, and dendritic orientation of these pleural COs match those in locusts (Hustert 1978). The other group is located in the medio-ventral region of abdominal sternites (Fig. 6i), termed ventral COs (indicated by white arrow, Fig. 6j). Short ligaments of ventral COs (approximately 100 μm) orient posteriorly to attach to the surface of fat body cells (Fig. 6j).

Central projections of COs

Vibration- and sound-sensitive CO neurons are known to project to a specific neuropil, the medial ventral association center (mVAC). The area of the mVACs relative to the ganglion in stink bugs was smaller than those in tympanate insects such as cicadas (Wohlers et al. 1979) and crickets (Wohlers and Huber 1985).

Stink bug Anterograde labeling of the FCO/SGO nerves in pro, meso and metathoracic legs (n=5 for each leg) consistently showed that these afferents supply axon terminals ipsilaterally in the dorso-lateral neuropil, the neuropil lateral to the mVAC (lateral association center, Pflüger et al. 1988), and the central region of the mVAC in pro, meso, metathoracic neuromeres, respectively (Fig. 7a-d, g, h). Hair receptors intermingling in the FCO/SGO nerves project almost exclusively to the lateral ventral association center (lVAC, Pflüger et al. 1988), as indicated by asterisks (Figs. 7b, d, h, j). A singly stained mesothoracic FCO neuron originating from the proximal region of the ventral scoloparium (Fig. 7e) has an axonal morphology similar to that of metathoracic FCO neurons that are sensitive to tibial extension in locusts (Matheson, 1992). The two mesothoracic SGO afferents, revealed by anterograde labeling of the SGO nerve, provide a few collaterals in the dorso-lateral neuropil and primary branches projecting to the central region of the mVAC (Fig. 7f, n=2). One thicker SGO afferent (red, Fig. 7f) provides axon terminals slightly ventrally to those of the other afferent (blue, Fig. 7f) in the mVAC. The branches projecting to the mVAC are more abundant in FCO/SGO afferents than in SGO afferents solely (compare Fig. 7g, h with Fig. 7i, j), suggesting that five to six additional afferents, very likely originating from the dorsal scoloparium, supply axon terminals to the mVAC.

Anterograde labeling of the tymbal nerve showed that individual neurons of the tymbal CO exhibit intersegmental projections (n=12). All four afferents provide dense arborizations primarily in the dorsal region of the mVAC in the metathoracic neuromere (magenta, Figs. 8b and S6; Figs. S2l). Three of them further ascend axons to provide axon terminals in homologous regions of the mVAC in meso (Figs. 8e and S2k), prothoracic (Figs. 8d and S2j), subesophageal neuromeres (Figs. 8c and S2i), two of which finally terminate in the antennal mechanosensory and motor center (Kristoffersen et al., 2008) of the brain (Figs. 8c and magenta arrows, S2h, i). Some short collaterals are also seen between these neuromeres (indicated by yellow arrow, Fig. 8e). Two afferents have descending axons to provide short collaterals in abdominal neuromeres (indicated by white arrow, Fig. 8e).

Anterograde labeling of the descending connective showed that abdominal CO afferents have two distinct morphologies: extensive projections (cyan, Fig. 8f) and localized projections (red, Fig. 8f). Anterograde labeling of a single abdominal nerve at

different proximo-distal levels further confirmed that extensive projections and localized projections are possessed by pleural COs and ventral COs, respectively (Fig. S3c-h). Two ipsi and contralateral pleural COs originating from the same abdominal segment show somewhat different projection patterns (Fig. S3h). Anterograde labeling of a sensory branch containing hair receptor axons in the fifth abdominal segment revealed their exclusive projections to the lateral ventral association center (Fig. S3a, b), as shown in locusts (Pflüger et al. 1981; Pflüger et al. 1988).

Similar to the tymbal CO, four pleural COs exhibit intersegmental projections; one afferent terminates in the central ganglion, and two terminate in the prothoracic ganglion and the remaining one projects up to the antennal mechanosensory and motor center of the brain (green, Fig. 8a-e). The ventral COs comprising six to eight afferents provide short collaterals in the lateral association center and dense arborizations in the dorso-lateral region of the mVAC of the metathoracic neuromere (Fig. S3e, f). Both pleural COs and ventral COs have additional short collaterals in abdominal neuromeres.

To compare projection fields of different COs in the mVAC, differential anterograde labeling in different combinations of the tymbal nerve, descending connectives (containing abdominal COs), and main leg nerve (containing FCO afferents) was performed. The afferents of four pleural COs (green, Fig. 8a-e) resemble those of the tymbal CO (magenta, Fig. 8a-e) in that they have intersegmental projections primarily in the dorsal region of the mVACs. Three differences, however, were noted: 1) The tymbal CO axons are thicker (about 1.2 μm) than pleural CO axons (about 0.8 μm), resulting in larger terminal varicosities in the mVAC (Figs. 8c-e), 2) tymbal COs tend to have axon terminals more closely to the midline compared to pleural COs (Fig. 8d, e), 3) the tymbal CO afferents have a few collaterals in the ventral region in addition to the dorsal region of the metathoracic mVAC, resulting in more extensive arborizations than the pleural CO afferents (Fig. 8b). Axon terminals of the FCO/SGO, tymbal CO/pleural COs, and ventral COs consistently occupy progressively more dorsal regions of the mVAC with some spatial overlapping (Fig. 8b, j, l, n, p).

Moreover, differential anterograde labeling of the antennal nerve and the tymbal nerve revealed that descending axons of presumed Johnston's organ (JO; Jerum and Pabst, 1996) afferents (green, Fig. 9) and ascending axons of the tymbal CO (magenta, Fig. 9) take different but close trajectories. Presumed JO afferents give rise to axon terminals in the dorsal region of the antennal mechanosensory and motor center of the

brain (Kristoffersen et al., 2008) and descend toward abdominal neuromeres by providing collaterals almost exclusively to the mVAC in each neuromere. Some overlap between axon terminals of presumed JO and those of the tymbal CO was evident in the brain (Fig. 9g), subesophageal (Fig. 9h, i), thoracic (Fig. 9j-l), and abdominal neuromeres (Fig. 9l), but presumed JO terminals in thoracic and abdominal neuromeres are generally located dorso-laterally to projection fields made by tymbal CO terminals (Fig. 9j-l).

Cicada Firstly, anterograde labeling of pro, meso and metathoracic FCO/SGO nerves showed that FCO and SGO afferents terminated in the dorso-lateral neuropil and the lateral association center but lacked axon terminals in the mVACs of pro, meso metathoracic neuromeres (Fig. 10a-d, n=3 for each). Several branches that superficially invade the lateral region of the mVAC are located just anterior and posterior to the mVAC (Figs. 10b, c, g and S7). Anterograde labeling of the SGO nerve in pro and mesothoracic legs showed that two SGO afferents primarily terminate in the lateral association center just lateral to the mVAC (Fig. 10e-h, n=3 for each). Hair receptors intermingling in the FCO nerves project almost exclusively to the lateral ventral association center (lVAC, Pflüger et al. 1988), as indicated by asterisks (Fig. 10 b-d and f).

Differential anterograde labeling of the auditory nerve (magenta, AN), the tensor nerve (green, TeN), and contralateral main leg nerve (green, MLN) showed that COs innervated by the auditory nerve and tensor nerve project almost exclusively to mVACs in the thoracic, abdominal and subesophageal neuromeres but that COs innervated by the auditory nerve terminate more dorsally than do COs innervated by the tensor nerve in the metathoracic neuromeres (Figs. 10i-n and S7), as shown in 17-year cicadas (Wohlers et al. 1979). A much smaller number of afferents (white arrow, Fig. 10i) ascend to provide short collaterals in the mesothoracic (Fig. 10k), prothoracic, and subesophageal neuromeres. Whereas COs innervated by the auditory nerve are limited to the ipsilateral neuromeres, COs innervated by the tensor nerve have some branches beyond the midline (white arrow, Fig. 10l, m). Several fibers originating from the auditory nerve and tensor nerve largely intermingle in the mVACs of the mesothoracic and abdominal neuromeres (Fig. 10k, n).

Discussion

Our comprehensive mappings of putative vibration-sensitive COs in hemipteran insects have demonstrated that in contrast to largely modified peripheral structures of COs, the central projections to serially homologous neuropils are similar to those in other insects, supporting the view of Boyan (1993) that the neuropilar organization is more conserved compared to the peripheral sensory system. The conservation of the mVAC is attributable, at least partly, to the fact that communications using vibratory signals are widespread from hemimetabolous to holometabolous insects (Virant-Doberlet and Čokl 2004; Cocroft and Rodriguez 2005). Our study therefore provides new insights into information processing of substrate vibration from comparative view points.

Peripheral structure of COs

The peripheral structure of COs in stink bugs has unique features that have not been reported in other insects. First, all of the COs that were studied lack the cuticular apodeme elongated from the proximal tibia. Second, the number of sensory neurons is greatly reduced compared to orthopteran COs, which are usually equipped with up to several hundred sensory neurons (Braünig et al. 1981; Matheson and Field 1990; Nishino 2000). Third, there are direct anatomical links between the attachment cells of COs and various tissues, such as specialized tendons, muscles, septa, and fat body cells. In contrast, the ligaments interconnecting peripheral tissues and sensory neurons are simple and uniform (Doolan and Young 1981; Michel et al. 1983). These findings suggest that frequency filtering of COs relies greatly on the resonant property of peripheral tissues. This is reasonable given that measurements of local mechanical properties of the body surface, which have transmission properties that are different from those of substrate vibrations, are particularly important for small insects to attain directional information (Cocroft et al. 2000).

FCO The FCO in stink bugs is characterized by its distal location of scoloparia in the femur. The lateralization of sensory neurons may facilitate segregation of bilateral sensory input and availability of directional cue in vibration source detection. In addition to this function, we propose that the direct insertion of attachment cells to peripheral tissues at short distances allows fast proprioceptive and exteroceptive mediation, thereby helping faithful transduction of the temporal sequence of “songs”,

because faster mechanical displacement of the ligaments must override the delay in conduction of action potentials due to the distal shift of sensory neurons. Indeed, distal shift of FCOs to different degrees has been found in plant-dwelling insects that have developed vibrational communications such as lacewings (Lipovsek et al. 1999; Taki et al. 2005) and *Mantophasma* (Eberherd et al. 2011). The decrease of sensory neurons in hemipteran FCOs enables maintenance of relatively large individual sensory cell bodies and axons thereby maintaining fast conduction velocity in unmyelinated axons.

The location, cell clustering manner, cellular displacements according to tibial positions, and dendritic morphologies collectively suggest that the ventral and dorsal scoloparia in stink bugs are homologous to the ventral and dorsal scoloparia, respectively, in stick insects (Kittmann and Schmitz 1992) and crickets (Nowel et al. 1995; Nishino 2000) and the distal and proximal scoloparia, respectively, in locusts (Burns 1974). The latter scoloparium has been suggested to participate preferentially in vibration detection rather than mediation of slow and large tibial movements (Field and Pflüger 1989).

The association of the stink bug FCO with the TEPS may contribute to accurate mechanical transduction of tibial movement and position. Due to the connection of the ventral ligament with the TEPS, rolling of the ligament into the F-T joint is hampered by the TEPS. This may allow precise measurement of F-T joint angle via an axial displacement of the ventral ligament. Different sites of attachment cells on the TEPS might underlie the rage fractionation mechanism that is achieved by connections of attachment cells to different points on the cuticular apodeme in locusts (Shelton et al. 1992) and crickets (Nowel et al. 1995).

The question arises as to why the dorsal ligament is attached to the accessory extensor muscle but not to the cuticle, since direct connections between the ligament and muscles have not been reported in other insect groups (Field and Matheson 1998). It could be presumed that dorsal scoloparium neurons are able to detect active muscle tension, such as isometric muscle contraction. Caution is, however, needed because the motoneuronal innervation to the AEM is rather feeble and the attachment site of the dorsal ligament is free from the innervation. The accessory muscle may be selected as the “static region” to achieve isolation of vibratory signals from proprioceptive signals mediated by tibial movement. The relative incompliance of dorsal scoloparium neurons to tibial movement compared to ventral scoloparium neurons may support this view.

Tymbal CO and pleural CO The tymbal CO contains four sensory neurons, whereas pleural COs each contain only one sensory neuron. Due to the close association with the tracheal muscle, the pleural CO is assumed to monitor its movements. The morphology of afferents strongly suggested that the tymbal CO is derived from pleural COs, possibly through the fusion of the two abdominal segments. This evolutionary scheme amazingly parallels that of tympanal organs in locusts and bladder grasshoppers in that both organs are derived from pleural COs as precursors, concomitant with augmentation of sensory neurons (Halax et al. 1988; van Staaden and Römer 1998).

The tymbal CO is closely appositioned to tymbal muscles and distally linked with fat body cells just beneath the ventral cuticle, suggesting its involvement in both monitoring of tymbal movement and detection of external vibration. Fat body cells, which are rich in lipids, are obviously more elastic and softer than the cuticle, and this feature might be suitable for low frequency filtering as dominant frequencies of tymbal sound lie in low and narrow frequency ranges, 80-120 Hz in *N. viridula* (Čokl et al. 2000). In wetas, lipid-synthesizing cells in the olivarius organ are located close to the tympanal chordotonal organ (Lomas et al. 2012). Removal of these cells resulted in a significant deficit of auditory sensitivity (Lomas et al. 2012). Since fat body cells are ubiquitous in the body lumen of stink bugs, these cells might globally affect the efficacy of vibration transmission of COs distributed in the body (Field and Matheson, 1998), though further investigation of this possibility is needed.

Functional layering of the mVAC

Our study revealed that the mVAC, conserved from hemimetabolous to holometabolous insects (Boyan 1993; Lakes-Harlan et al. 1999), is the primary target of CO axons in hemipteran insects. The mVAC has layering structures according to carrier frequencies of sensory afferents, suggesting its importance for analyzing vibration/sound frequencies. For instance, afferents tuning to sounds of higher frequencies tend to project to the more posterior region in the mVAC of the locust (Halax et al. 1988). In katydids, distal sensory neurons, which respond best to high frequencies, terminate at the posterior end and proximal receptors, tuned to progressively lower frequencies, terminate at progressively anterior sites in the mVAC (Oldfield 1988; Römer et al. 1988; Stumpner 1996; Stölting and Stumpner 1998). On the other hand, dorsal scoloparium neurons of the FCO project to the dorsal region of

the mVAC, segregated from termination fields of tympanal organ afferents that project to more ventral regions in crickets (Nishino 2000) and primitive orthopteran insects, wetas (Nishino 2003).

Similar functional subdivision appears to be the case for hemipteran mVACs. As summarized in Figure 11a-d, axon terminals of the FCO/SGO, tymbal CO/pleural COs, JO, and ventral COs in stink bugs progressively occupy more dorso-lateral regions in mVACs with some spatial overlap. These projection patterns suggest not only divergence of afferents from different COs for discriminating vibrational frequencies but also convergence of a specific subset of different locational COs for analysis of similar frequencies. The latter is especially important for enhancing directional sensitivity because it provides a neural substrate for temporal summation of signals representing mechanical properties on the body surface, which change according to vibrational direction (Cocroft et al. 2000).

The conserved structure of the mVAC allows assessment of the functional aspects of COs with respect to sensory neuronal and interneuronal physiologies in other insects. Given that SGO neurons generally tune to frequencies higher than dominant frequencies (around 120 Hz) used for ordinary vibrational communications (Čokl 1983; Čokl and Virant-Doberet 2003; Čokl 2008) while JO afferents generally tune to lower frequencies (60-100 Hz) in *N. viridula* (Jerum and Čokl 1996), the more dorso-lateral region of the mVAC in hemipteran insects appears to serve for processing of vibrations with lower frequencies. Similar dendritic organization of vibration-responsive interneurons according to their tuning frequencies has been reported in the atympanate ensiferan *Troglophilus neglectus* (Stritih 2009). In *N. viridula*, transverse views of vibration-responsive interneurons (Zorović et al. 2008; Zorović 2011) have not been provided, making it difficult to compare these morphologies with morphologies of afferents because projection differences at the antero-posterior axis between different COs are ambiguous.

Our results also revealed unique morphology of tymbal CO, two neurons of which supplied axon terminals from abdominal neuromeres to the brain neuropil, the most extensive projections ever known in insect COs. These afferents provide axonal arborizations in mVACs but no branches in the dorso-lateral neuropils that are implicated in motor control (Pflüger et al. 1988), suggesting the tymbal CO's extensive influence on vibrational processing rather than reflexive local motor control. A

comparison between self-emitting tymbal oscillation and recurrent vibration detected by COs distributed throughout the body would be important for coordination of song emission, and thus extensive central projections are suited for rapid intersegmental coordination as well as higher-order integration for generating song commands. Investigation of tuning properties of the tymbal CO is indispensable to evaluate this possibility.

Evolutional implication of hemipteran COs from comparative viewpoints

Our study highlightened the morphological differences between the stink bug COs and cicada COs, despite their close phylogenetic relation (Cui et al. 2013; Wang et al. 2015). Indeed, the bauplan for emitting vibration/sound, peripheral nerve innervation and location of sense organs appear to be shared by stink bugs and cicadas (Fig. 11e, f). However, a closer look at the distal structures of COs revealed that that the dorsal ligament in the cicada FCO is fused into the ventral ligament unlike the stink bug counterpart, which is separately attached to the accessory extensor muscle. Possibly reflecting this, one scolopidium in the dorsal scoloparium of stink bugs appeared to be associated with the ventral ligament in cicadas. Mesothoracic and metathoracic SGO neurons in cicadas were attached to a septum in the hemolymph channel via a short ligament, differing from the stink bug SGO neurons that attach to the dorso-distal region of the femur via an elongated ligament. Moreover, the FCO and SGO afferents in cicadas are devoid of terminations in the mVAC. These observations suggest that some modifications in distal structures and afferent morphology occurred in leg COs during the evolutional transition from the predominant use of substrate vibration to airborne sound for conspecific communication.

Intriguingly, two pairs of dorsal scoloparium neurons and two SGO neurons presumably associated with vibration detection still exist in cicadas. Given the lack of spatial overlap in afferents between FCO/SGO and tympanal COs, both organs appear to be functionally segregated to avoid jamming of airborne sound processing with substrate vibration processing. The airborne sound emitted by singing cicadas can be transmitted through the substrate, but its dominant frequency is close to that of the sound (Stölting et al. 2002). Therefore, the detection of substrate vibration accompanied by self-emitting sound signals appears to provide little value for intraspecific communications in cicadas. Hence, we suspect that leg vibration detectors in cicadas

may tune to lower frequencies of substrate vibrations, e.g. those generated by approaching predators, which would be important for their survival.

Adoption of airborne sound as a communication tool is advantageous over substrate vibration because of better directivity of sound. The enlargement of body mass and elaboration of the sound production apparatus (tymbal) would allow cicadas to opt for sound instead of substrate vibration for conspecific communications, with elaboration of pre-existing sensory systems (Fig. 11). It is noteworthy that similar evolutional transition has been exerted independently on sensory systems in different insect orders, such as orthopteran insects (Boyan 1993; Stumpner and von Helversen 2001), cockroaches (Shaw, 1994), and flies (Lakes-Harlan et al. 1999). In the future, it would be beneficial to investigate vibration receptors such as dorsal scoloparium neurons of FCOs and SGO neurons in primitive cicadas that predominantly use substrate vibrations for intraspecific communications (Claridges et al. 1999).

Acknowledgments

This work was supported by Innovative Materials Engineering Based on Biological Diversity in Grant-in-Aid for Scientific Research on Innovative Areas (project number: 80332477) to HN and TT, Council for Science, Technology and Innovation, Cross-ministerial Strategic Innovation Promotion Program to TT and Grant-in-Aid for JSPS Fellow (14J30005) and Young Scientists (B) (15K18618) to HM. We thank K. Katoh for collecting *L. bihamatus*, Dr. T. Ichikawa (Kyusyu University) for supplying *Z. atratus*, and Drs. T. Ishikawa (Tokyo University of Agriculture), Niels Skals (University of Copenhagen) and two anonymous reviewers for comments on the manuscript.

Table 1. Comparison of the numbers of sensory neurons in FCOs of the stink bug and cicada.

Insect	leg	Ventral scoloparium		Dorsal scoloparium neurons	Total number of neurons	n
		Proximal neurons	Distal neurons			
P. stali	pro	10	8	6	24	5
	meso	10	8	6	24	7
	meta	10	8	6	24	5
P. japonensis	pro	10	8	6	24	3
	meso	10	8	6	24	3
	meta	10	8	6	24	2
L. bihamatus	pro	12	8	4	24	4
	meso	12	8	4	24	5
	meta	12	8	4	24	4
T. nigracosta	pro	12	8	4	24	1
	meso	12	8	4	24	2
	meta	12	8	4	24	1

No sexual difference was detected in male and female FCOs of stink bugs and cicadas.

References

Bacon JP, Altman JS (1977) A silver intensification method for cobalt-filled neurons in wholemount preparations. Brain Res 138:359-363

Bennet-Clark HC (1998) Size and scale constraints in insect sound communication. Philos Trans R Soc Lond B 353:407-419

Boyan GS (1993) Another look at insect audition: The tympanic receptors as an evolutionary specialization of the chordotonal system. J Insect Physiol 39:187-200

Bräunig P, Hustert R, Pflüger HJ (1981) Distribution and specific central projections of mechanoreceptors in the thorax and proximal leg joints of locusts. Cell Tissue Res 216:57-77

Bräunig P (1982) Strand receptors with central cell bodies in the proximal leg joints of orthopterous insects. Cell Tissue Res 222:647-654

Burns MD (1974) Structure and physiology of the locust femoral chordotonal organ. J Insect Physiol 20:1319-1339

Claridge MF, Morgan JC, Moulds MS (1999) Substrate-transmitted acoustic signals of the primitive cicada, *Tettigarcta crinita* Distant (Hemiptera Cicadoidea, Tettigarctidae). J Nat Hist 33:1831-1834

Cocroft RB, Tieu TD, Hoy RR, Miles RN (2000) Directionality in the mechanical response to substrate vibration in a treehopper (Hemiptera: Membracidae: *Umbonia crassicornis*). J Comp Physiol A 186:695-705

Cocroft RB, Rodríguez RL (2005) The behavioral ecology of insect vibrational communication. Bioscience 55:323-334

Čokl A (1983) Functional properties of vibroreceptors in the legs of *Nezara viridula* (L.). (Heteroptera, Pentatomidae). J Comp Physiol A 150:261-269

Čokl A (2008) Stink bug interaction with host plants during communication. J Insect Physiol 54:1113–1124

Čokl A, Virant-Doberlet M, Stritih N (2000) Temporal and spectral properties of the songs of the southern green stink bug *Nezara viridula* (L.) from Slovenia. Pflüger Arch Eur J Physiol 439:168-170

Čokl A, Virant-Doberlet M (2003) Communication with substrate-borne signals in small plant-dwelling insects. Annu Rev Entomol 48:29-50

Čokl A, Virant-Doberlet M, Zorović M. (2006) Sense organs involved in the vibratory

communication of bugs. In: Drosopoulos S, Claridge MF (eds) Insect sounds and communication: physiology, behaviour, ecology and evolution. CRC Press, Boca Raton, FL:. pp 71-80.

Cui Y, Xie Q, Hua J, Dang K, Zhou J, Liu X, Wang G, Yu X, Bu W (2013) Phylogenomics of Hemiptera (Insecta: Paraneoptera) based on mitochondrial genomes. Syst Entomol 38:233-245

Debaisieux P (1935) Organes scolopidiaux des pattes d'insectes. I. Lépidoptères et Trichoptères. La Cellule 44:271-314

Devetak D, Pabst MN (1994) Structure of the subgenual organ in the green lacewing *Chrysoperla carnea*. Tissue Cell 26:249-257.

Debaisieux P (1938) Organes scolopidiaux des pattes d'insectes. II. La Cellule 47:77-202

Doolan JM, Young D (1981) The organization of the auditory organ of the bladder cicada, *Cystosoma saundersii*. Philos Trans R Soc Lond B 291: 525-540

Eberhard MJB, Lang D, Metscher B, Pass G, Picker MD, Wolf H (2010) Structure and sensory physiology of the leg scolopidial organs in Mantophasmatodea and their role in vibrational communication. Arthropod Struct Dev 39:230-241

Evans PD, O'Shea M (1978) The identification of an octopaminergic neurone and the modulation of a myogenetic rhythm in the locust. J Exp Biol 73:235-260

Field LH, Burrows M (1982) Reflex effects of the femoral chordotonal organ upon leg motor neurones of the locust. J Exp Biol 101:265-285

Field LH, Pflüger HJ (1989) The femoral chordotonal organ: a bifunctional orthopteran (*Locusta migratoria*) sense organ? Comp Biochem Physiol 93A:729-743

Field LH, Matheson T (1998) Chordotonal organs of insects. Adv Insect Physiol 27:1-228

Furth DG, Suzuki K (1990) Comparative morphology of the tibial flexor and extensor tendons in insects. Syst Entomol 15:433-441

Gogala M, Čokl A, Drašler K, Blaževič A (1974) Substrate-borne sound communication in Cydnidae (Heteroptera). J Comp Physiol 94:25-31

Halex H, Kaiser W, Kalmring K (1988) Projection areas and branching patterns of the tympanal receptor cells in migratory locusts, *Locusta migratoria* and *Schistocerca gregaria*. Cell Tissue Res 253:517-528

Hayashi K (1985) Alternative mating strategies in the water strider *Gerris elongates*

(Heteroptera, Gerridae). Behav Ecol Sociobiol 16:301-306
Hill PSM (2008) Vibrational communication in animals. Harvard University Press, Cambridge, MA.
Hoffmann T, Koch UT, Bässler U (1985) Physiology of the femoral chordotonal organ in the stick insect *Cuniculina impigra*. J Exp Biol 114:207-223
Hustert R (1978) Segmental and intersegmental projections from primary fibres of insect mechanoreceptors. Cell Tissue Res 194:337-351
Jeram S, Čokl A (1996) Mechanoreceptors in insects: Johnston's organ in *Nezara viridula* (L.) (Pentatomidae, Heteroptera,). Pflügers Arch 431:281-282
Jeram S, Pabst MA (1996) Johnston's organ and central organ in *Nezara viridula* (L.) (Heteroptera, Pentatomidae). Tissue Cell 28:227-235
Kavčič A, Čokl A, Laumann RA, Blassioli-Moraes MC, Borges M (2013) Tremulatory and abdomen vibration signals enable communication through air in the stink bug *Euschistus heros*. PLoS ONE 8:e56503
Kittmann R, Schmitz J (1992) Functional specialization of the scoloparia of the femoral chordotonal organ in stick insects. J Exp Biol 173:91-108
Koczor S, Čokl A (2014) Percussion signals of *Lygus rugulipennis* Poppius (Heteroptera: Miridae) Cent Eur J Biol 9:543-549
Kristoffersen L, Hansson BS, Anderbrandt O, Larsson MC (2008) Aglomerular hemipteran antennal lobes–basic neuroanatomy of a small nose. Chem Senses 33:771-778
Lakes-Harlan R, Stölting H, Stumpner A (1999) Convergent evolution of insect hearing organs from a preadaptive structure. Proc R Soc Lond B 266:1161-1167
Lakes-Harlan R, Strauß J (2014) Functional morphology and evolutionary diversity of vibration receptors in insects. In: Cocroft RB, Gogala M, Hill PSM, Wessel A (eds) Studying Vibrational Communication. Springer, Heidelberg New York Dordrecht London, pp 277-302
Laumann RA, Kavčič A, Moraes MCB, Borges M, Čokl A (2013) Reproductive behaviour and vibratory communication of the neotropical predatory stink bug *Podisus nigrispinus*. Physiol Entomol 38:71-80
Lipovšek L, Pabst MA, Devetak D (1999) Femoral chordotonal organ in the legs of an insect, *Chrysoperla carnea* (Neuroptera). Tissue Cell 31:154-162
Lomas KF, Greenwood DR, Windmill JFC, Jackson JC, Corfield J, Parsons S (2012)

Discovery of a lipid synthesising organ in the auditory system of an insect. PLoS ONE 7:e51486.

Matheson T (1990) Responses and locations of neurones in the locust metathoracic femoral chordotonal organ. J Comp Physiol A 166:915-927

Matheson T, Field LH (1990) Innervation of the metathoracic femoral chordotonal organ of *Locusta migratoria*. Cell Tissue Res 259:551-560

Matheson T (1992) Morphology of the central projections of physiologically characterised neurones from the locust metathoracic femoral chordotonal organ. J Comp Physiol A 170:101-120

McBrien HL, Millar JG (2003) Substrate-borne vibrational signals of the consperse stink bug (Hemiptera: Pentatomidae). Can Entomol 135:555-567

Michel K, Amon T, Čokl A (1983) The morphology of the leg scolopidial organs in *Nezara viridula* (L.) (Heteroptera, Pentatomidae). Rev Can Biol Exp 42:139-150

Michelsen A, Fink F, Gogala M, Traue D (1982) Plants as transmission channels for insect vibrational songs. Behav Ecol Sociobiol 11:269-281

Miklas N, Stritih N, Čokl A, Virant-Doberlet M, Renou M (2001) The influence of substrate on male responsiveness to the female calling song in *Nezara viridula*. J Insect Behav 14:313-332

Moraes MCB, Laumann RA, Čokl A, Borges M (2005) Vibratory signals of four Neotropical stink bug species. Physiol Entomol 30:175-188

Moran DT, Varela FJ, Rowley III JC (1977) Evidence for active role of cilia in sensory transduction. Proc Natl Acad Sci USA 74:793-797

Mukai H, Hironaka M, Tojo S, Nomakuchi S (2012) Maternal vibration induces synchronous hatching in a subsocial burrower bug. Anim Behav 84:1443-1448

Mukai H, Hironaka M, Tojo S, Nomakuchi S (2014) Maternal vibration: An important cue for embryo hatching in a subsocial shield bug. PLoS ONE 9:e87932

Nishino H (2000) Topographic mapping of the axons of the femoral chordotonal organ neurons in the cricket *Gryllus bimaculatus*. Cell Tissue Res 299:145-157

Nishino H (2003) Somatotopic mapping of chordotonal organ neurons in a primitive ensiferan, the New Zealand tree weta *Hemidenia femorata*: I. Femoral chordotonal organ. J Comp Neurol 464:312-326

Nishino H, Filed LH (2003) Somatotopic mapping of chordotonal organ neurons in a primitive ensiferan, the New Zealand tree weta *Hemideina femorata*: II. Complex tibial

organ. J Comp Neurol 464:327-342

Nomakuchi S, Yanagi T, Baba N, Takahira A, Hironaka M, Filippi L (2012) Provisioning call by mothers of a subsocial shield bug. J Zool 288:50-56

Nowel MS, Shelton PMJ, Stephen RO (1995) Functional organisation of the metathoracic femoral chordotonal organ in the cricket *Acheta domesticus*. J Exp Biol 198:1977-1988

Numata H, Kon M, Fujii H, Hidaka T (1989) Sound production in the bean bug, *Riptortus clavatus* Thunberg (Heteroptera: Alydidae). Appl Entomol Zool 24:169-173

Oldfield BP (1988) Tonotopic organization of the insect auditory pathway. Trends Neurosci 11:267-270

Pflüger HJ, Bräunig P, Hustert R (1981) Distribution and specific central projections of mechanoreceptors in the thorax and proximal leg joints of locusts. Cell Tissue Res 216:79-96

Pflüger HJ, Bräunig P, Hustert R (1988) The organization of mechanosensory neuropiles in locust thoracic ganglia. Philos Trans R Soc Lond B Biol Sci 321:1-26

Römer H, Marquart V, Hardt M (1988) Organization of a sensory neuropile in the auditory pathway of two groups of Orthoptera. J Comp Neurol 275:201-215

Shaw SR (1994) Detection of airborne sound by a cockroach'vibration detector': a possible missing link in insect auditory evolution J Exp Biol 193:13-47

Shelton PMJ, Stephen RO, Scott JJA, Tindall AR (1992) The apodeme complex of the femoral chordotonal organ in the metathoracic leg of the locust *Schistocerca gregaria*. J Exp Biol 163:345-358

Simmons P, Young D (1978) The tymbal mechanism and song patterns of the bladder cicada, *Cystosoma saundersii*. J Exp Biol 76:27-45

Stein W, Sauer AE (1999) Physiology and vibration-sensitive afferents in the femoral chordotonal organ of the stick insect. J Comp Physiol 184:253-263

Stölting H, Stumpner A (1998) Tonotopic organization of auditory receptors of the bushcricket *Pholidoptera griseoaptera* (Tettigoniidae, Decticinae). Cell Tissue Res 294:377-386

Stölting H, Moore TE, Lakes-Harlan R (2002) Substrate vibrations during acoustic signaling in the cicada *Okanagana rimosa*. J Insect Sci 2:2-7

Strauß J, Lakes-Harlan R (2013) Sensory neuroanatomy of stick insects highlights the evolutionary diversity of the orthopteroid subgenual organ complex. J Comp Neurol

521:3791-3803
Stritih N (2009) Anatomy and physiology of a set of low-frequency vibratory interneurons in a nonhearing ensiferan (*Troglophilus neglectus*, Rhaphidophoridae) J Comp Neurol 516:519-532
Stumpner A (1996) Tonotopic organization of the hearing organ in a bushcricket: physiological characterization and complete staining of auditory receptor cells. Naturwissenschaften 83:81-84
Stumpner A, Von Helversen D (2001) Evolution and function of auditory systems in insects. Naturwissenschaften 88:159-170
Taki H, Kuroki S, Nomura M (2005) Taxonomic diversity within the Japanese green lacewing, *Chrysoperla carnea* (Neuroptera: Chrysopidae), identified by courtship song analyses and crossing tests. J Ethol 23:57-61
Van Staaden MJ, Römer H (1998) Evolutionary transition from stretch to hearing organs in ancient grasshoppers. Nature 394:773-776
Virant-Doberlet M, Čokl A (2004) Vibrational communication in insects. Neotropical Entomol 33:121-134
Wang Y, Chen J, Jiang L-Y, Qiao G-X (2015) Hemipteran mitochondrial genomes: features, structures and implications for phylogeny. Int J Mol Sci 16: 12382-12404
Wohlers DW, Williams JLD, Huber F, Moore TE (1979) Central projections of fibers in the auditory and tensor nerves of cicadas (Homeoptera: Cicadidae). Cell Tissue Res 203:35-51
Wohlers DW, Huber F (1985) Topographical organization of the auditory pathway within the prothoracic ganglion of the cricket *Gryllus campestris* L. Cell tissue Res 239:555-565
Wolfrum U (1990) Actin filaments: the main components of the scolopale in insect sensilla. Cell Tissue Res 261:85-96
Yack J (2004) The structure and function of auditory chordotonal organs in insects. Micros Res Tech 63:315-337
Young D (1975) Chordotonal organs associated with the sound producing apparatus of cicadas (Insecta, Homoptera). Z Morph Tiere 81:111-135
Young D, Hill KG (1977) Structure and function of the auditory system of the cicada, *Cystosoma saundersii*. J Comp Physiol [A]117:23-45
Zorović M, Prešern J, Čokl A (2008) Morphology and physiology of vibratory

interneurons in the thoracic ganglia of the southern green stinkbug *Nezara viridula* (L.). J Comp Neurol 508:365-381

Zorović M (2011) Temporal processing of vibratory communication signals at the level of ascending interneurons in *Nezara viridula* (Hemiptera: Pentatomidae). PLoS ONE 6: e26843

Žunič A, Čokl A, Virant-Doberlet M, Millar JG (2008) Communication with signals produced by abdominal vibration, tremulation, and percussion in *Podisus maculiventris* (Heteroptera: Pentatomidae). Ann Entomol Soc Am 101:1169-1178

Zych AF, Mankin RW, Gillooly JF, Forman E (2012) Stridulation by *Jadera haematoloma* (Hemiptera: Rhopalidae): production mechanism and associated behaviors. Ann Entomol Soc Am 105:118-127

Figure Legends

Fig. 1 Structures of the femoral chordotonal organ (FCO) and subgenual organ (SGO) in stink bugs. **(a-c)** Three-dimensional reconstructions of the peripheral nerve innervation in the prothoracic leg of *P. stali*, viewed anteriorly (a) and medially (b), and two partly fused FCO scoloparia associated with the ventral ligament (VL) and the dorsal ligament (DL), viewed posteriorly (c). TEPS: tibial extensor pendant sclerite. (**d)** Chitin material enveloping the VL and DL, labeled by wheat germ agglutinin (WGA). (**e-g)** Two-dimensional stacks of optical sections showing the ventral scoloparium (VS) and dorsal scoloparium (DS) and four pairs of distally located sensory neurons (d1-d4) on the VL of *P. stali*, viewed anteriorly (e) and dorsally (f). Similar scoloparial location and nerve innervation are seen in *P. japonensis* (g). (**h-k)** Three-dimensional reconstructions of the ventral scoloparium neurons (green) and dorsal scoloparium neurons (magenta), viewed anteriorly (h) and dorsally (i). One pair of sensory neurons in each scoloparium showing two dendrites extending into a common scolopale cap (SC), viewed anteriorly (j) and dorsally (k). (**l-n)** Subgenual organ (SGO) in *P. stali*, showing two sensory neurons extending dendrites into different SCs (indicated by yellow arrows, l, m), and specialized muscle fibers (white arrows, l, m) of the retractor unguis. Scale bars: 100 μm in a and b; 50 μm in c-f, m and n; 20 μn in inset in e, h-k; 200 μm in g and l.

Fig. 2 Attachment sites of the ventral ligament (VL) and the dorsal ligament (DL) of the FCO in stink bugs. (**a, b)** Three-dimensional reconstruction of the distal femur, viewed anteriorly (a) and posteriorly (b) showing that the VL (magenta) attaches to the antero-dorsal site of the TEPS, while the DL (green) attaches to the mid-posterior region of the AEM. (**c, d)** The femoro-tibial joint fixed at full extension (c) and full flexion (d), showing axial displacement of the TEPS at approximately 100 μm via the distal extensor tendon (DET, shaded by red, c). (**e, f)** Silver-intensified peripheral nerves in the distal femur, showing innervation of the accessory extensor muscle (AEM, shaded by green). The AEM receives local innervation of a tributary of the dorsal branch of the extensor nerve (marked by blue arrows in inset, e) in the dorso-central region (e). The attachment site of the DL (indicated by a white arrow, f) is free from motoneuronal innervation. Scale bars= 50 μm in a,b, e, and f; 100 μm in c, d. 200 μm in

inset, c.

Fig. 3 Cellular displacements according to tibial positions in intact FCOs of stinkbugs. **(a, a', a", b, b', b", c, c', c", and d)** Mappings of cellular displacements of mesothoracic FCO neurons according to the three tibial positions (a-c) and measurements of distances of two distal pairs of neurons from the fixed point (d). Asterisks in d indicate statistical significances (one-way ANOVA with Tuckey's pairwise comparison).

Fig. 4 Structures of the FCO and SGO in cicadas. **(a, b**) Peripheral nerve innervation of the prothoracic FCO (yellow arrow, a) and metathoracic FCO (yellow arrow, b), showing their distal locations in the femur, similar to the stink bug FCOs. **(c-e)** Differential labeling of sensory neurons (magenta) and F-actin filaments (green) showing two pairs of dorsal scoloparium neurons (c, d) and nine pairs of ventral scoloparium neurons (c) including four pairs of distal neurons (d1-d4, inset) arrayed on the VL. Scolopale rods are particularly rich in F-actin filaments. The DL comprises two pairs of neurons (1, 2, in d) and parallel attachment cells (1, 2 in e). (**f, g**) Peripheral nerve innervation of the mesothoracic SGO (f) and prothoracic SGO (g), showing two sensory neurons with two scolopale caps (inset, f). The ligament of the meso- or metathoracic SGO attaches to a septum bridging between the cuticle and the trachea, while that of the prothoracic SGO attaches to the dorso-distal cuticle of the femur. Scs: scolplae caps; sep: septum. Scale bars= 1 mm in a, b; 100 μm in inset, c; 50 μm in c, e; 20 μm in d; 200 μm in f; 10 μm in inset, f; 500 μm in g.

Fig. 5 Differential labeling of sensory neurons (magenta) and F-actin filaments (green) in COs of different insects. (**a-m)** FCOs in the locust (a-c), cricket (d, e), stink bug (g-j), and tenebrionid beetle (k-m) and tympanal organ neurons in the cricket (f). The F-actin filaments in the dorsal scoloparium and dorsal ligament (white arrow, a, b, d, k) are richer than those in the ventral scoloparium and ventral ligament (yellow arrow, a, b, d, k). Three pairs of DS neurons are detectable in two stink bug species (g, j). Scolopale caps (SCs) of DS neurons (g, j, m) are wider than those of VS neurons (h, j, l). **(n-p)** Distal region of attachment cells showing the coiled cuticular apodeme in the cricket (n) and rod-like cuticular apodeme in the locust (o) and tenebrionid beetle (p). Scale bars=

50 μm in a-e, i, k, n-p; 20 μm in f-j, l, m.

Fig. 6 Structure of the tymbal CO and abdominal COs in the stink bug *P. stali*. **(a, b)** Photomicrograph of the proximal abdomen viewed posteriorly (a) and its drawing using *camera lucida* (b), showing two muscles and the tymbal CO innervated by the tymbal nerve (TyN). The tymbal CO is anteriorly backed by the tymbal muscle. **(c, d)** Silver-intensified tymbal CO showing four sensory neurons (white arrows, c) proximally attached to the cuticular ridge between the metathorax and the fused abdominal segment and distally attached to fat body cells via the ligament (d). **(e)** Unfixed fat body cells in the ventral region of the body lumen, stained with toluidine blue. **(f-j)** Peripheral innervation of the descending connective (DC). The DC innervates V-VIII segments. Yellow circles in (f) indicate attachment sites of two tymbal COs. Each hemisegment contains one pleural CO neuron (g, h) close to the spiracle muscle (indicated by blue arrows, f) and one ventral CO (I, j), as exemplified in the 5th abdominal segment. Scale bars= 1 mm in a, b, f, i; 50 μm in c; 100 μm in d, e, g, j; 20 μm in h.

Fig. 7 Convergent projections of FCO and SGO in the stink bug *P. stali*. (**a, b)** Single mesothoracic FCO afferent (left) and metathoracic FCO/SGO afferents (right) viewed ventrally (a) and anteriorly (b). In this and the following figures, the medial ventral association center (mVAC) is outlined by a broken line and the midline is indicated by a broken straight line. Hair receptors project to the lateral ventral association center, separated from the mVAC (indicated by asterisks, b; see also Fig. S3a, b). Note single fibers ascending and descending from the metathoracic FCO projection field. (**c, d)** Prothoracic FCO/SGO afferents ventrally (c) and anteriorly (d). In this specimen, a strand receptor (SR) is stained (Braünig et al. 1982). (**e, f)** Drawings of a mesothoracic VS afferent (e, drawn from a) and two mesothoracic SGO afferents (f, drawn from i). The two SGO afferents project to slightly different ventro-dorsal planes of the mesothoracic neuromere. (**g-j)** Mesothoracic FCO viewed ventrally (g) and anteriorly (h) and two SGO afferents viewed ventrally (i) and dorsally (j), showing that projections to the mVAC are more abundant in the FCO/SGO than in SGO afferents solely. Scale bars= 100 μm in a, g, i; 50 μm in b-f, h, j.

Fig. 8 Partly overlapping projection fields of the tymbal CO, abdominal COs and FCOs in the stink bug *P. stali*. (**a-e)** Anterograde labeling of the descending connective (green) and tymbal nerve (magenta) viewed ventrally (a, c, d, e) and anteriorly (b), showing that tymbal CO (tyCO) afferents are more ventral than the abdominal CO (abCO) afferents in the metathoracic neuromere (b) but are largely intermingling in the subesophageal (c), pro- (d), and mesothoracic neuromeres (e). **(f)** Two populations of abdominal COs discriminated by signal intensity, showing extensive (cyan) and localized projections (red) in the metathoracic neuromere. See Fig. S3 for projection patterns of individual abdominal COs. (**g, h)** Anterograde labeling of the pro, meso, and metathoracic main leg nerves (MLNs, (green) and the tymbal nerve (TyN, magenta). (**i-n)** Three-dimensional reconstructions of FCO afferents (green) and tymbal CO afferents (magenta), showing that the tymbal CO provide terminals more profusely in the dorsal region of the mVAC compared to FCO afferents in the pro- (i, j), meso- (k, l) and metathoracic neuromeres (m, n), although some spatial overlap is evident. (**o, p)** Three-dimensional reconstructions of FCO afferents (blue), tymbal CO afferents (magenta) and abdominal CO afferents (green) in the metathoracic neuromere. The sectioning levels in j, l, and n are shown in b and C. Scale bars= 100 μm in a, g, h; 50 μm in b-e, i, j, o, p; 20 μm in f, k-n.

Fig. 9 Partly overlapping projections of Johnston's organ (JO) and the tymbal CO in the stink bug *P. stali*. (**a)** Low magnified confocal stack of anterograde labeling of the antennal nerve (AN, green) and the tymbal nerve (TyN, magenta). (**b-f)** High magnified confocal stack of the presumed JO afferents (green) and the tymbal CO afferents (magenta) in the brain (b), subesophageal ganglion (SEG, c), and pro (d), meso, meta (e) and abdominal neuromeres (f). (**g-l)** Three-dimensional reconstructions showing that ascending afferents of the tymbal CO and descending afferents of presumed JO contact each other in the postero-lateral region of the antennal mechanosensory and motor center (b,g) and their axon terminals are largely overlapping in each neuromere (h-l). The sectioning levels in h and j are shown in a. Scale bars = 200 μm in a; 20 mm in b-l.

Fig. 10 Intrasegmental projections of FCOs and SGOs and intersegmental projections of auditory COs in the cicada. See Fig. 4a, b for locations of the FCO nerves and Fig. 11c for locations of the auditory nerve (AN) and tensor nerve (TeN). (**a-d)** Anterograde

labeling of pro-, meso- and matathoracic FCO nerves in the same specimen, viewed ventrally (a) and anteriorly (b-d), showing that FCO projections are far lateral to the midline, not entering the mVAC. The sectioning levels in b-d are shown in a. (**e-h**) Anterograde labelings of the prothoracic and mesothoracic SGO nerves, showing that two afferents primarily terminate in the lateral association center located laterally to the mVAC in the prothoracic neuromere (e,f) and the mesothoracic neuromere (g,h). (**i-n)** Anterograde labeling of the auditory nerve (AN, magenta, left) and tensor nerve (TeN, green, left) and the metathoracic MLN (magenta, right), showing that auditory nerve afferents are more dorsally located than tensor nerve afferents in the mVAC and that MLN afferents (including metathoracic FCO afferents) do not enter the mVAC. The sectioning levels in l-n are shown in i. Note that several afferents ascend to meso, pro and subesophageal neuromeres (white arrows, e). Scale bars = 100 μm in a, e, f and 50 μm in b-d and g-j.

Fig. 11 Summary of projection patterns of different COs in hemipteran insects. (**a, b)** Projections of the FCO, SGO, tymbal CO, JO and two groups of abdominal COs in stink bugs, viewed ventrally (a) and anteriorly (b). (**c, d)** Projections of the FCO and two groups of auditory COs in cicadas, viewed ventrally (a) and anteriorly (b). Insets in b and d show peripheral locations of the mesothoracic FCO and SGO in stink bugs (b) and cicadas (d). The mVAC in stink bugs is less developed than that in tympanate cicadas. **(e, f)** Anterograde stainings of tensor nerve and auditory nerve in the cicada and homologous nerves in the stink bug, showing much decreased but largely overlapping projections of the stink bug tymbal CO and nearby pleural COs. Scale bars = 100 μm in a; 200 μm in b.

Fig. S1 Staining procedures. (**a, b)** Examples of retrograde staining of the main leg nerve (MLN) with microruby in *P. stali* (a) and $NiCl_2$ (reacted with rubeanic acid) in *P. Japonensis* (b). (**c)** An example of anterograde staining of three peripheral nerves with microruby to label their axonal projections in the central ganglion (CG). (**d)** An unfixed central ganglion reacted with rubeanic acid in which the tymbal nerve (left) and the metathoracic MLN (right) were retrogradely labeled with $NiCl_2$. PG: prothoracic ganglion. **(e-g)** Fat body cells in the body lumen of *P. stali* at low (e), mid (f), and high magnifications (g, stained with toluidine blue). Scale bars= 1 mm in a, b, e; 500 μm in c,

f; 200 μm in d; 20 μm in g.

Fig. S2 Anterograde labeling of four nerves innervating the proximal region of the abdomen. (**a)** Nomenclature of peripheral nerves in the central ganglion (CG). (**b-g)** Projections of N1 (b), N2 (c), and N3 (d) indicating one or two CO afferents projecting to the mVAC for each nerve. They have no axons that ascend to the brain. **(h-l)** Projections of the tymbal nerve (TN) showing four CO afferents (indicated by black arrows in h and i) in prothoracic (j), mesothoracic (k), and metathoracic neuromeres (l). Two CO afferents have collaterals that terminate in the antennal mechanosensory and motor center in the brain (indicated by yellow arrows in h and i). See Fig. 7 for details. Scale bars= 100 μm in b-g; 200 μm in h, i; 50 μm in j-l.

Fig. S3 Projection patterns of two populations of abdominal COs. (**a, b)** Anterograde staining of the most peripheral dorsal branch of the primary nerve in the fifth abdominal segment, showing projections of hair receptors confined to the most ventral neuropil. (**c, d)** Anterograde staining of the nerve branch innervating the pleural CO in the fifth (left) and sixth abdominal segments showing a single afferent that has collaterals in the dorsal region of mVACs in the meso- and metathoracic neuromeres (d) and terminate in the prothoracic neuromere. (**e, f**) Anterograde staining of the distal tip of the nerve containing the pleural CO and more proximal nerve containing pleural and ventral COs, revealing that the proximal abdominal CO has localized branches in the metathoracic neuromere (left). Scale bars = 100 μm in a, c, e, g; 50 μm in b, d, f, h.

Fig. S4 Retrograde labeling of FCO neurons (magenta) and surrounding structures (green) i*n P. stali,* viewed anteriorly.

Fig. S5 Retrograde labeling of FCO neurons (magenta) and F-action filaments (green) in *P. Japonensis* showing different scolopale structures of dorsal scoloparium neurons (surrounded by white line) and ventral scoloparium neurons.

Fig. S6 Anterograde labeling of the main metathoracic leg nerve (green) and the tymbal nerve (magenta) in *P. stali* showing projections of FCO/SGO afferents (green) and tymbal CO afferents (magenta) to the mVAC, viewed anteriorly.

Fig. S7 Anterograde labeling of the auditory nerve (left, magenta) and tensor nerve (left, green) and the main metathoracic leg nerve (right, green) in *L. bihamatus* showing that auditory nerve afferents are more dorsally located than tensor nerve afferents in the mVAC and that metathoracic FCO afferents do not enter the mVAC.

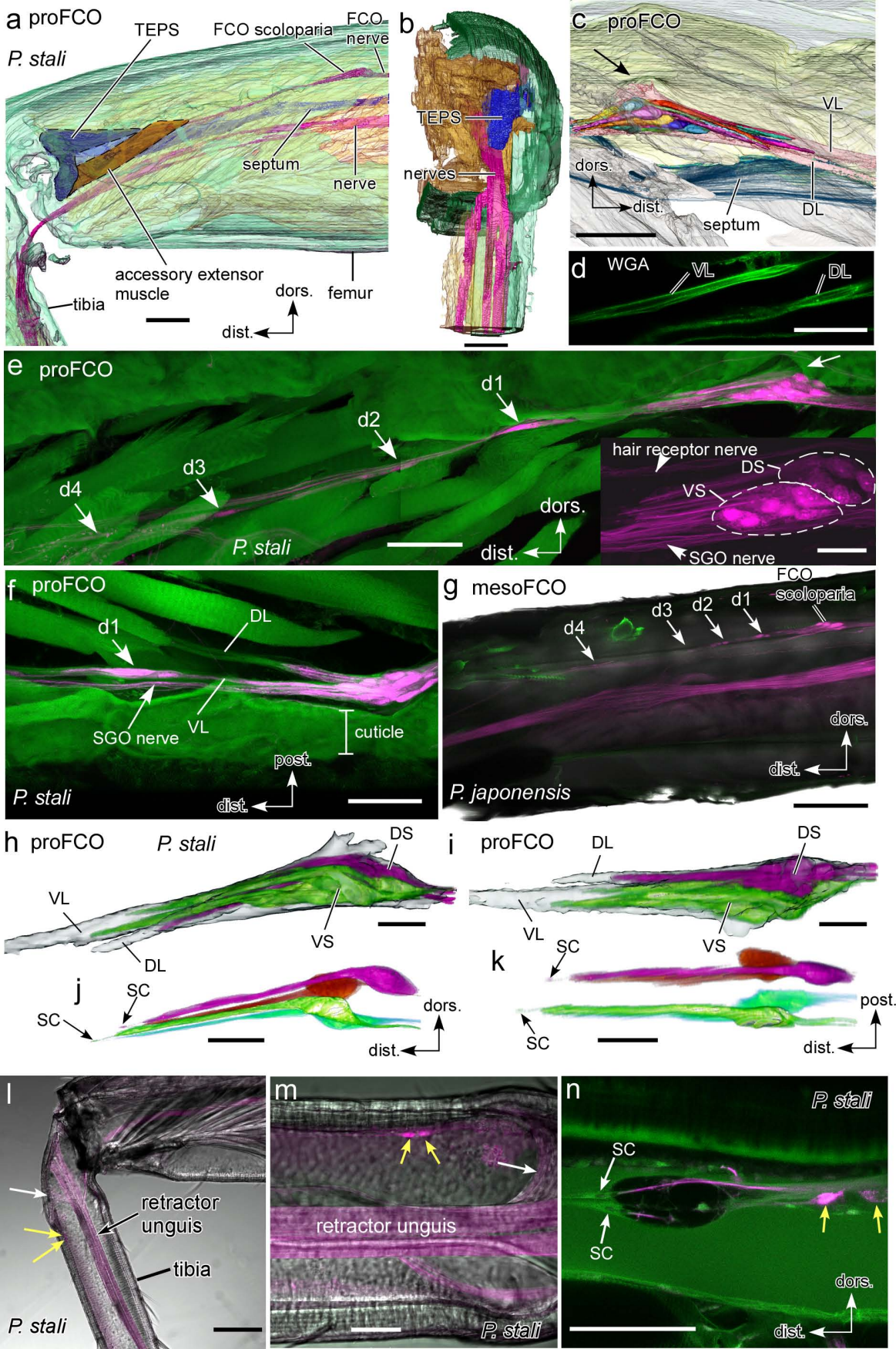
a proFCO
P. stali
TEPS
FCO scoloparia
FCO nerve
septum
nerve
accessory extensor muscle
tibia
dors.
dist.
femur
b
TEPS
nerves
c proFCO
VL
dors.
dist.
DL
septum
d WGA
VL
DL
e proFCO
d1
d2
d3
d4
P. stali
dors.
dist.
hair receptor nerve
DS
VS
SGO nerve
f proFCO
d1
DL
SGO nerve
VL
cuticle
post.
dist.
P. stali
g mesoFCO
FCO scoloparia
d4
d3
d2
d1
dors.
dist.
P. japonensis
h proFCO
P. stali
DS
VL
VS
DL
i proFCO
DL
DS
VL
VS
j
SC
SC
dors.
dist.
k
SC
SC
post.
dist.
l
retractor unguis
tibia
P. stali
m
retractor unguis
P. stali
n
P. stali
SC
SC
dors.
dist.

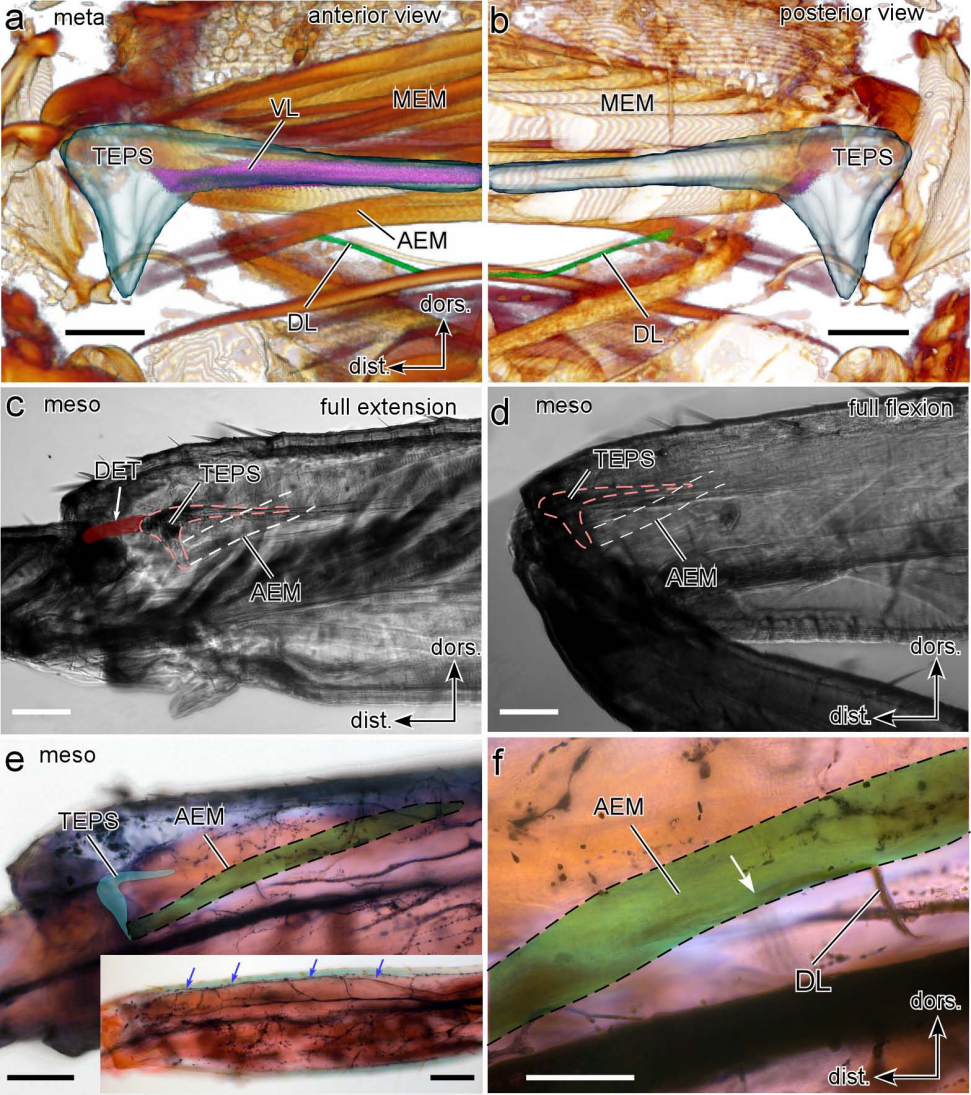
a
meta
anterior view
VL
MEM
TEPS
AEM
DL
dors.
dist.
b
posterior view
MEM
TEPS
DL
c
meso
full extension
DET
TEPS
AEM
dors.
dist.
d
meso
full flexion
TEPS
AEM
dors.
dist.
e
meso
TEPS
AEM
f
AEM
DL
dors.
dist.

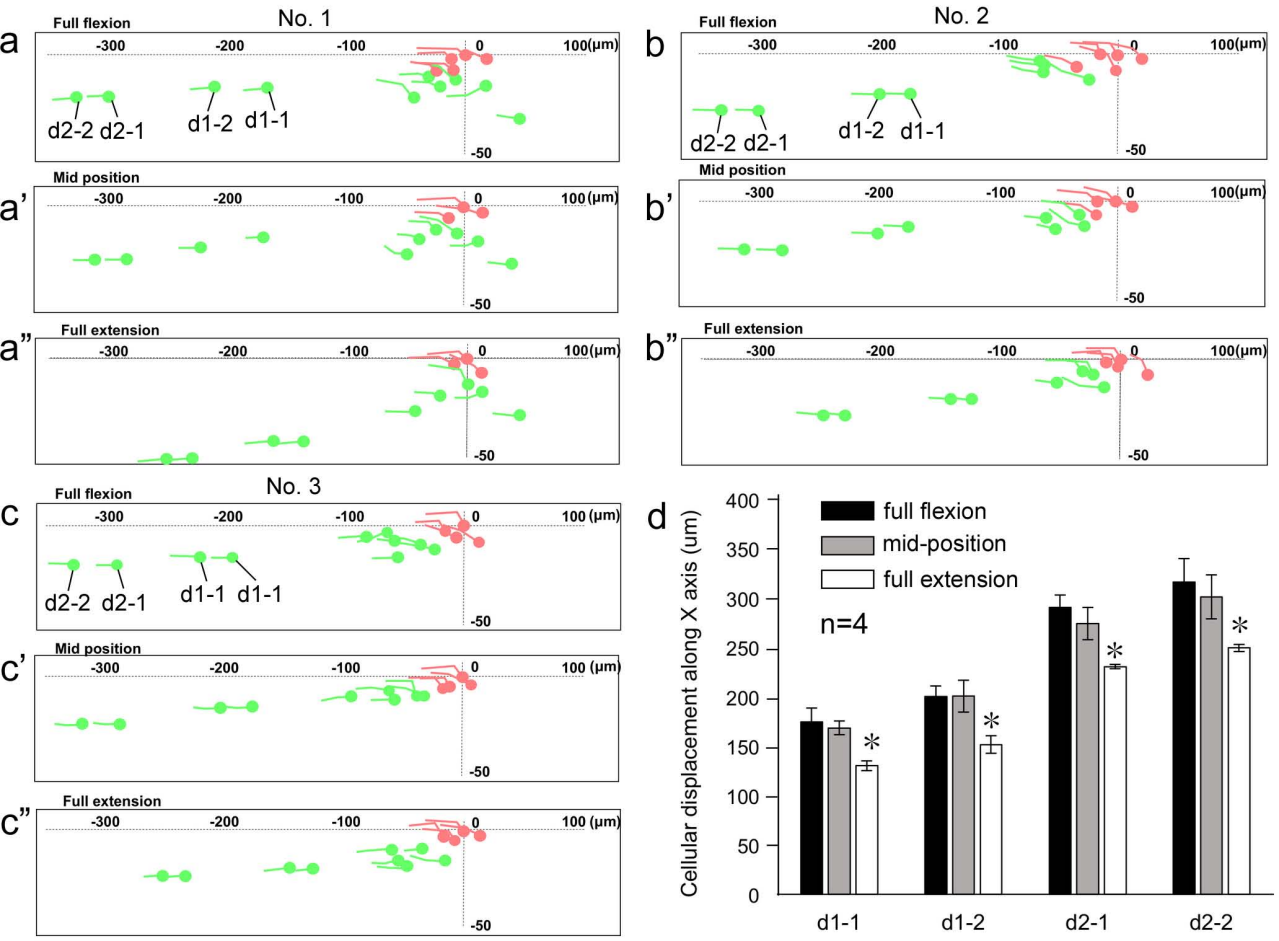
a
Full flexion
No. 1
-300
-200
-100
0
100(μm)
d2-2 d2-1
d1-2 d1-1
-50
a'
Mid position
a"
Full extension
b
No. 2
b'
b"
c
No. 3
d2-2 d2-1
d1-1 d1-1
c'
c"
d
full flexion
mid-position
full extension
n=4
Cellular displacement along X axis (um)
400
350
300
250
200
150
100
50
0
d1-1
d1-2
d2-1
d2-2
*

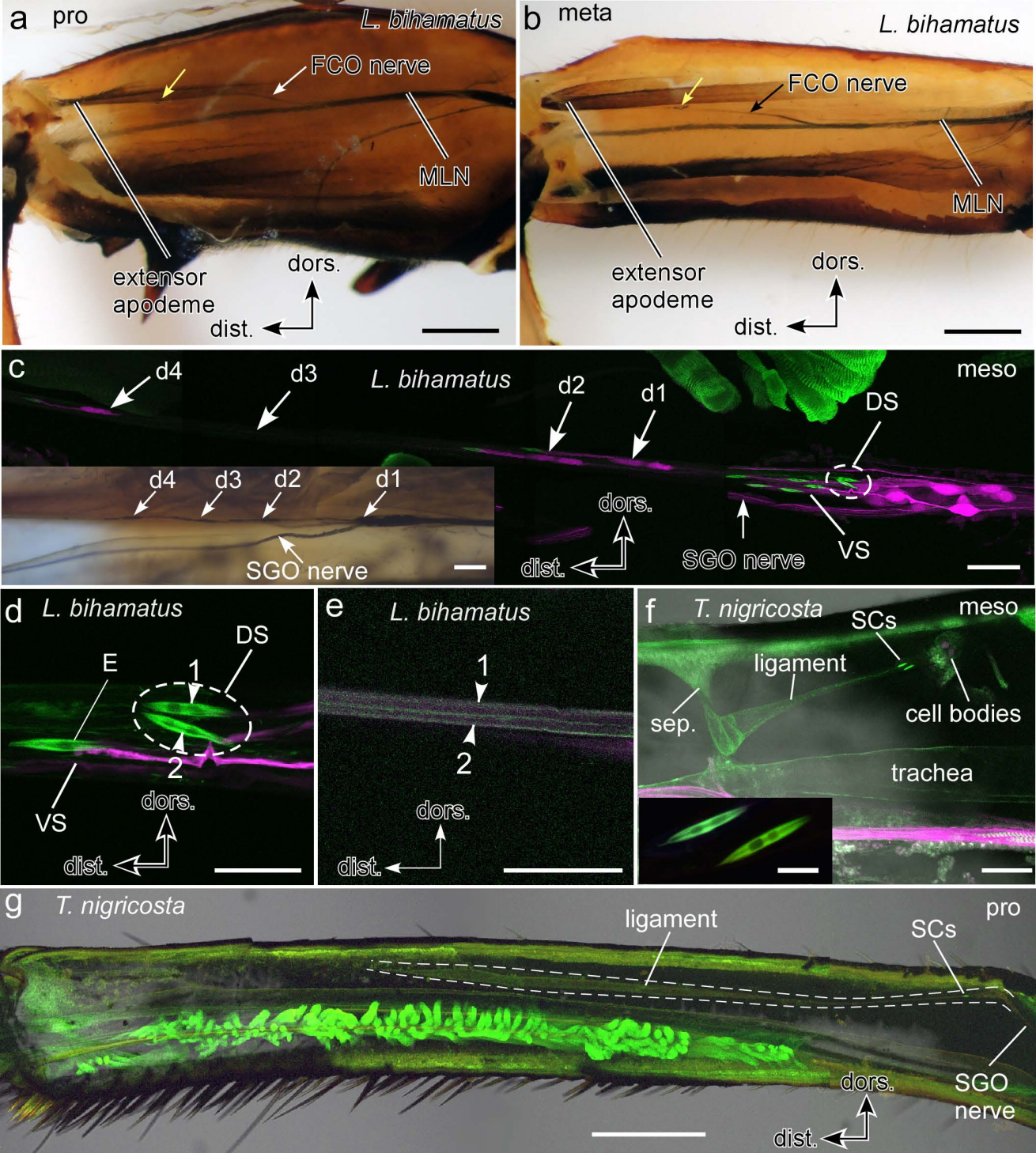
a
pro
L. bihamatus
FCO nerve
MLN
extensor apodeme
dors.
dist.
b
meta
L. bihamatus
FCO nerve
MLN
extensor apodeme
dors.
dist.
c
d4
d3
L. bihamatus
d2
d1
meso
DS
d4
d3
d2
d1
SGO nerve
dors.
dist.
SGO nerve
VS
d
L. bihamatus
DS
E
1
2
VS
dors.
dist.
e
L. bihamatus
1
2
dors.
dist.
f
T. nigricosta
SCs
meso
ligament
sep.
cell bodies
trachea
g
T. nigricosta
ligament
SCs
pro
dors.
dist.
SGO nerve

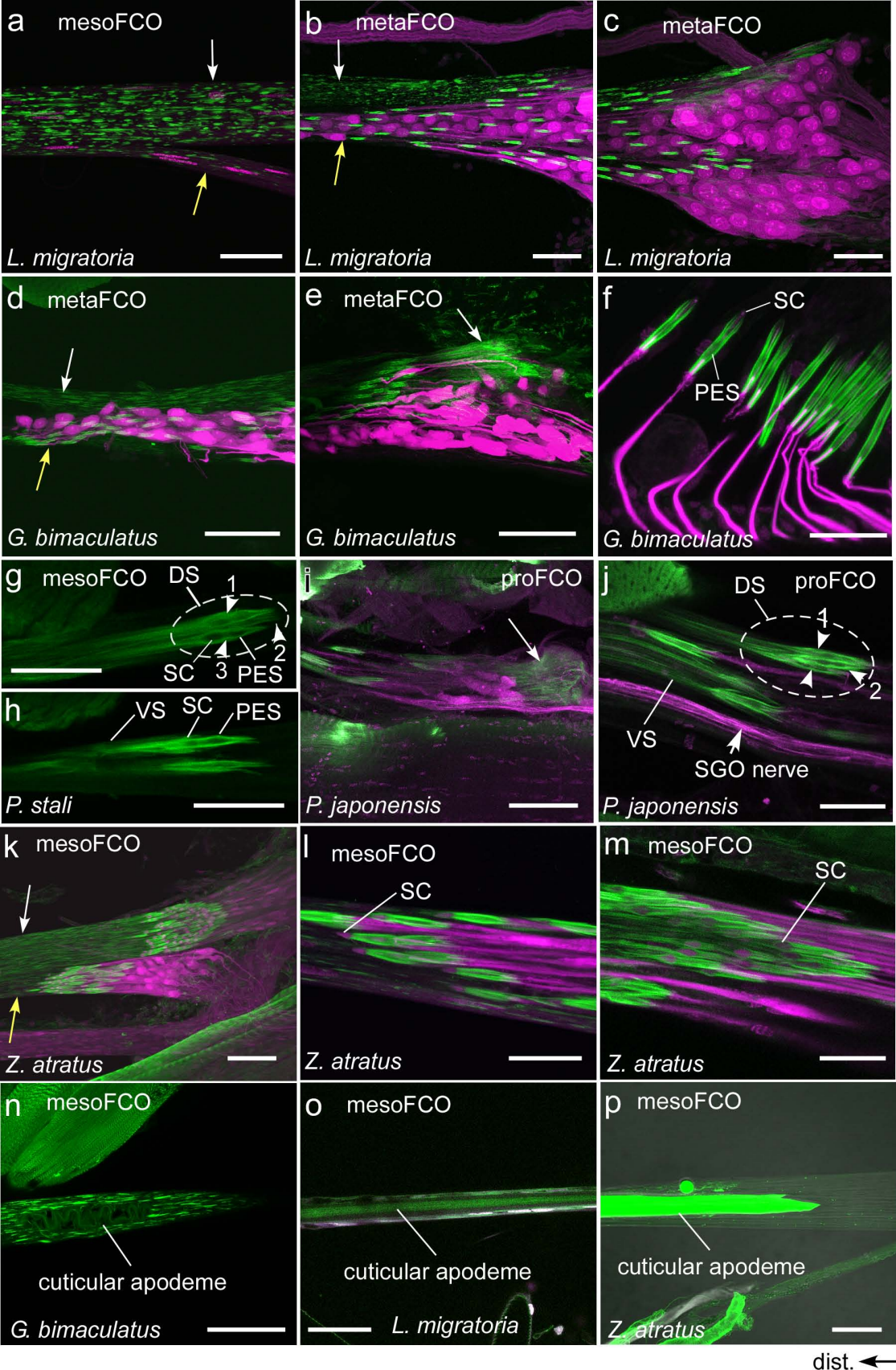
a
mesoFCO
L. migratoria
b
metaFCO
L. migratoria
c
metaFCO
L. migratoria
d
metaFCO
G. bimaculatus
e
metaFCO
G. bimaculatus
f
SC
PES
G. bimaculatus
g
mesoFCO
DS
1
2
SC
3
PES
h
VS
SC
PES
P. stali
i
proFCO
P. japonensis
j
DS
proFCO
1
2
VS
SGO nerve
P. japonensis
k
mesoFCO
Z. atratus
l
mesoFCO
SC
Z. atratus
m
mesoFCO
SC
Z. atratus
n
mesoFCO
cuticular apodeme
G. bimaculatus
o
mesoFCO
cuticular apodeme
L. migratoria
p
mesoFCO
cuticular apodeme
Z. atratus
dors.
dist.

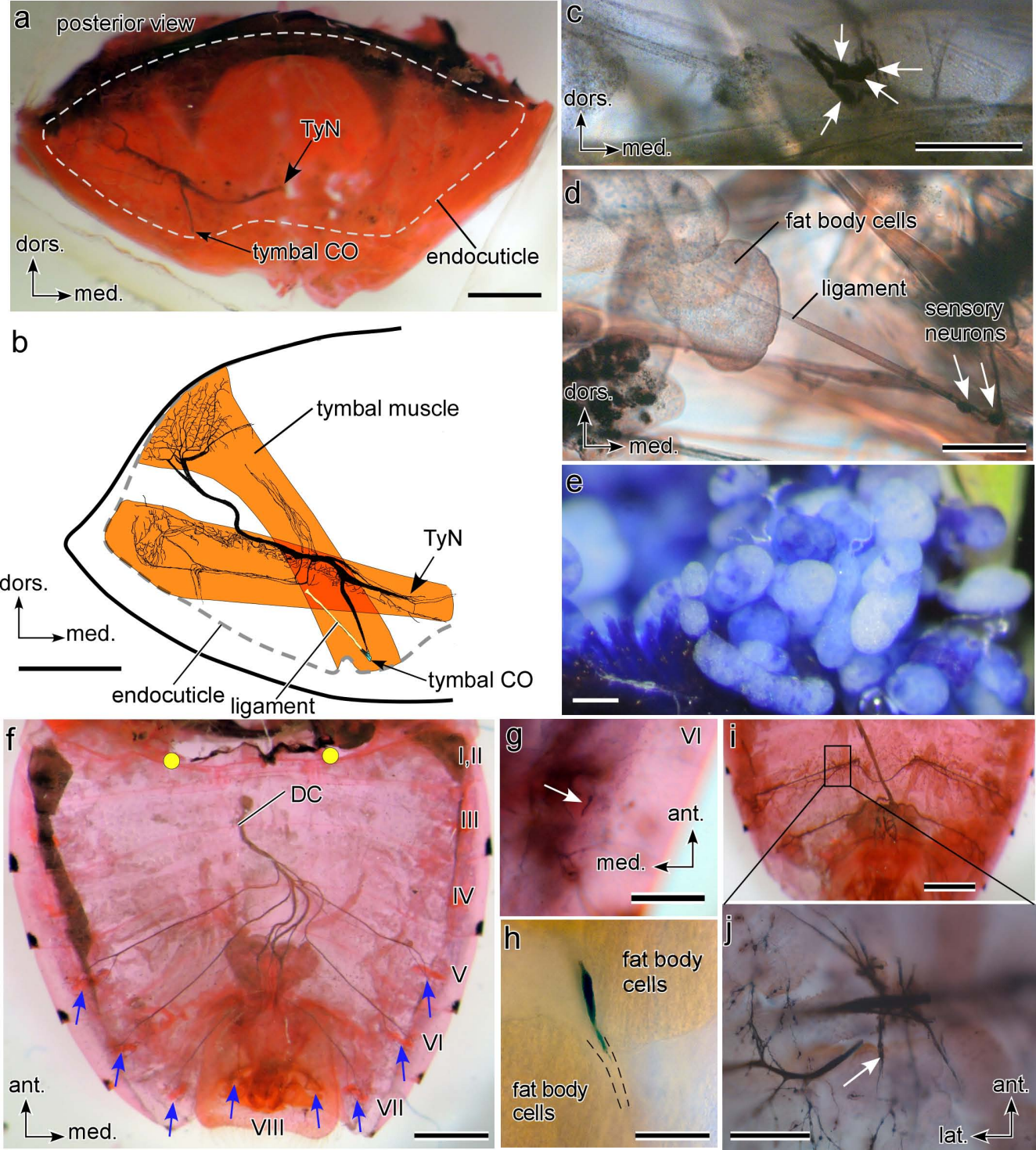
a
posterior view
TyN
tymbal CO
endocuticle
dors.
med.
b
tymbal muscle
TyN
dors.
med.
endocuticle
ligament
tymbal CO
c
dors.
med.
d
fat body cells
ligament
sensory neurons
dors.
med.
e
f
I,II
DC
III
IV
V
VI
VII
VIII
ant.
med.
g
VI
ant.
med.
h
fat body cells
fat body cells
i
j
ant.
lat.

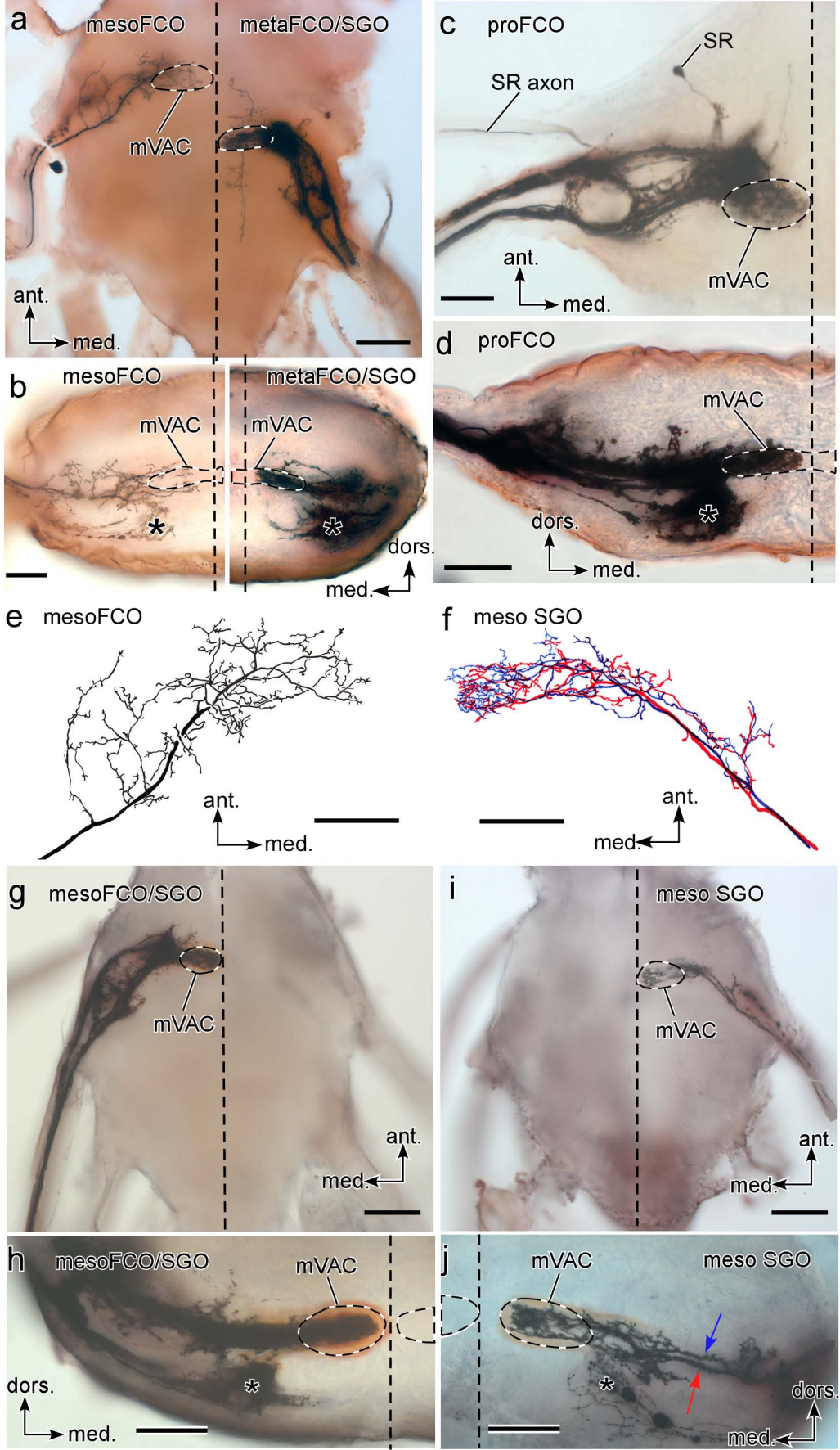
a
mesoFCO
metaFCO/SGO
mVAC
ant.
med.
b
mesoFCO
metaFCO/SGO
mVAC
mVAC
dors.
med.
c
proFCO
SR
SR axon
ant.
med.
mVAC
d
proFCO
mVAC
dors.
med.
e
mesoFCO
ant.
med.
f
meso SGO
ant.
med.
g
mesoFCO/SGO
mVAC
ant.
med.
i
meso SGO
mVAC
ant.
med.
h
mesoFCO/SGO
mVAC
dors.
med.
j
mVAC
meso SGO
dors.
med.

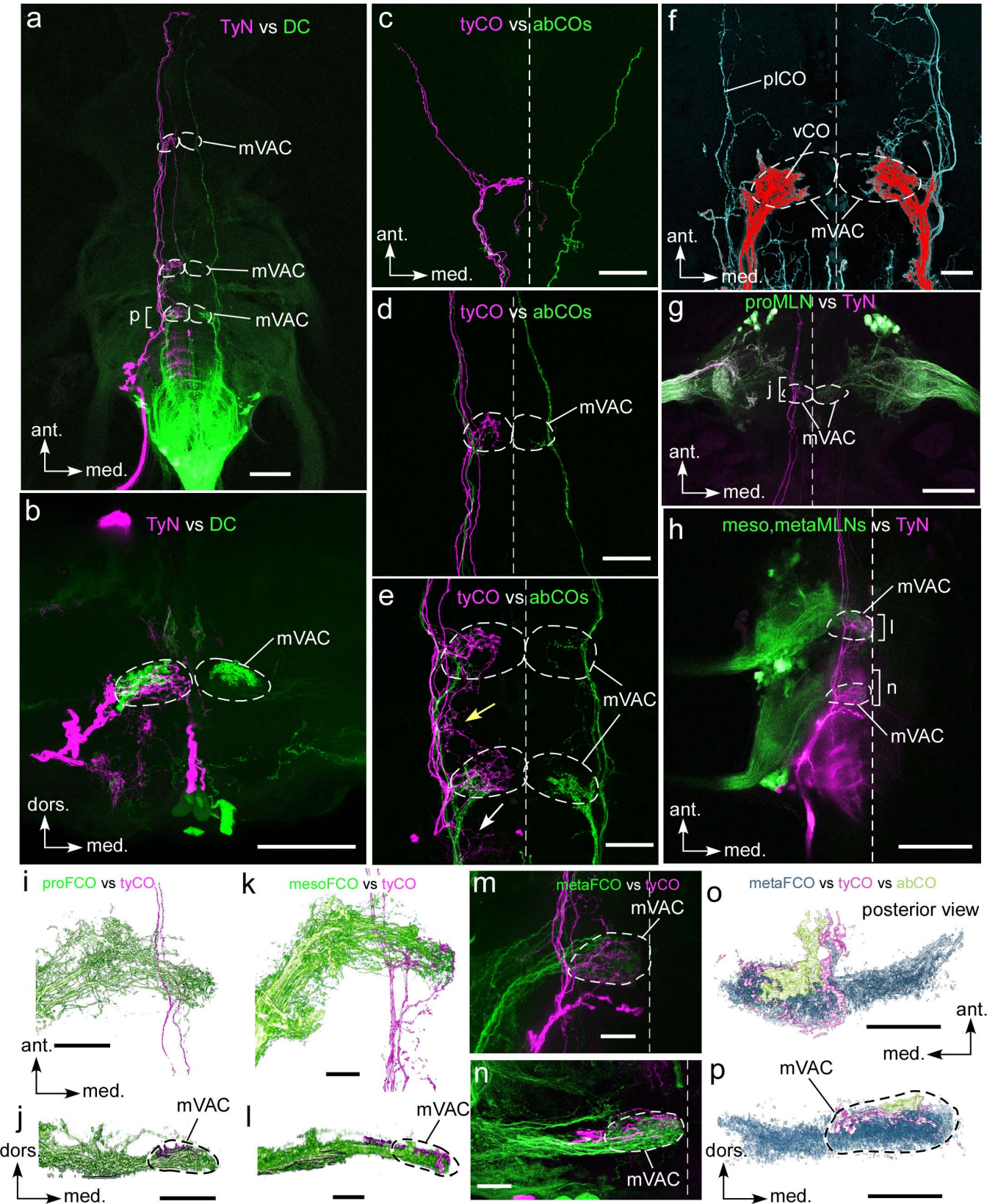
a
TyN vs DC
mVAC
mVAC
p [
mVAC
ant.
med.
b
TyN vs DC
mVAC
dors.
med.
c
tyCO vs abCOs
ant.
med.
d
tyCO vs abCOs
mVAC
e
tyCO vs abCOs
mVAC
f
plCO
vCO
mVAC
ant.
med.
g
proMLN vs TyN
j [
mVAC
ant.
med.
h
meso,metaMLNs vs TyN
mVAC
l
n
mVAC
ant.
med.
i
proFCO vs tyCO
ant.
med.
j
mVAC
dors.
med.
k
mesoFCO vs tyCO
l
mVAC
m
metaFCO vs tyCO
mVAC
n
mVAC
o
metaFCO vs tyCO vs abCO
posterior view
ant.
med.
p
mVAC
dors.
med.

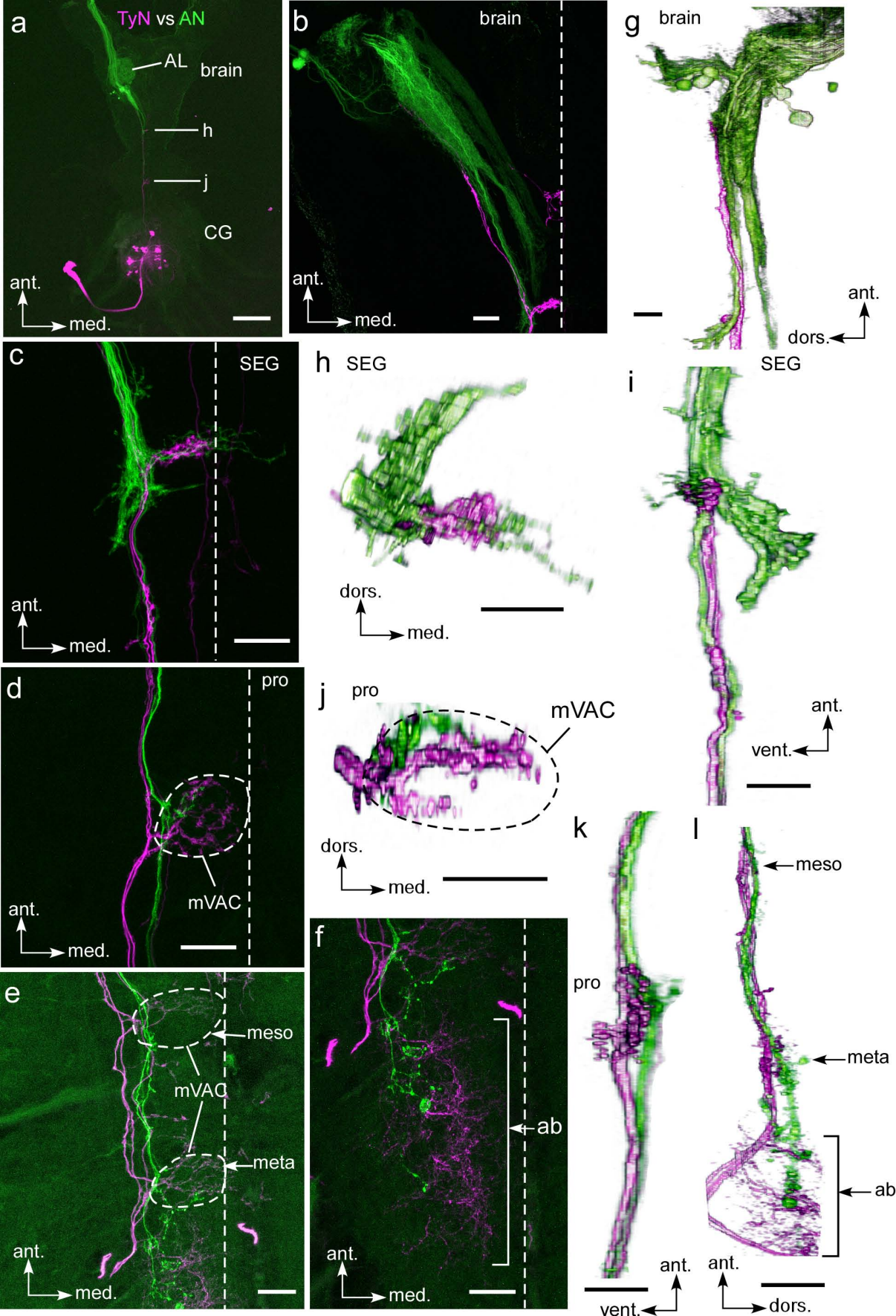
a
TyN vs AN
AL
brain
h
j
CG
ant.
med.
b
brain
ant.
med.
g
brain
ant.
dors.
c
SEG
ant.
med.
h
SEG
dors.
med.
i
SEG
ant.
vent.
d
pro
mVAC
ant.
med.
j
pro
mVAC
dors.
med.
k
pro
ant.
vent.
l
meso
meta
ab
ant.
dors.
e
meso
mVAC
meta
ant.
med.
f
ab
ant.
med.

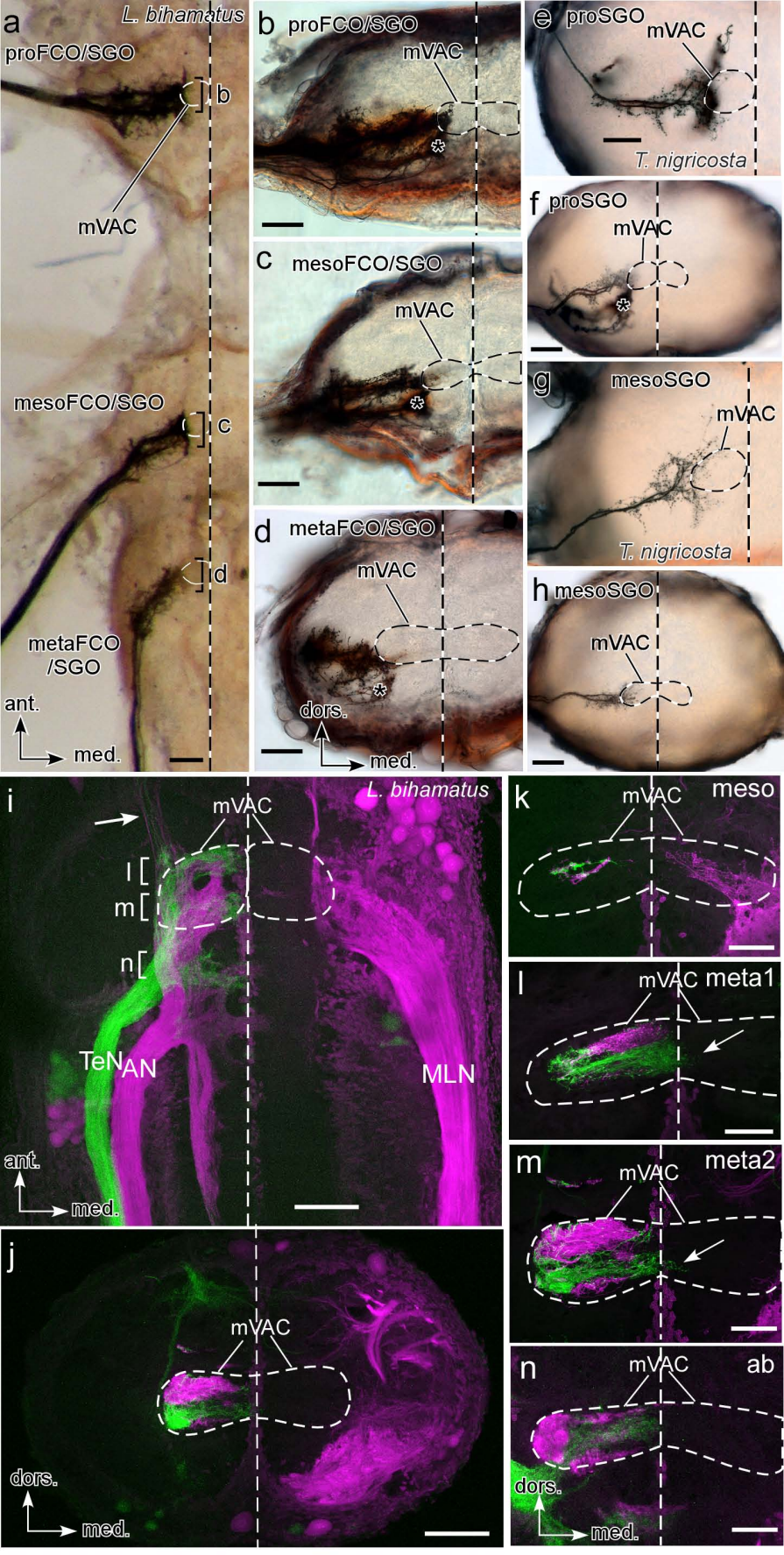
a
L. bihamatus
proFCO/SGO
b
mVAC
mesoFCO/SGO
c
d
metaFCO
/SGO
ant.
med.
b proFCO/SGO
mVAC
c mesoFCO/SGO
mVAC
d metaFCO/SGO
mVAC
dors.
med.
e proSGO
mVAC
T. nigricosta
f proSGO
mVAC
g mesoSGO
mVAC
T. nigricosta
h mesoSGO
mVAC
i
L. bihamatus
mVAC
l
m
n
TeN
AN
MLN
ant.
med.
j
mVAC
dors.
med.
k
mVAC
meso
l
mVAC
meta1
m
mVAC
meta2
n
mVAC
ab
dors.
med.

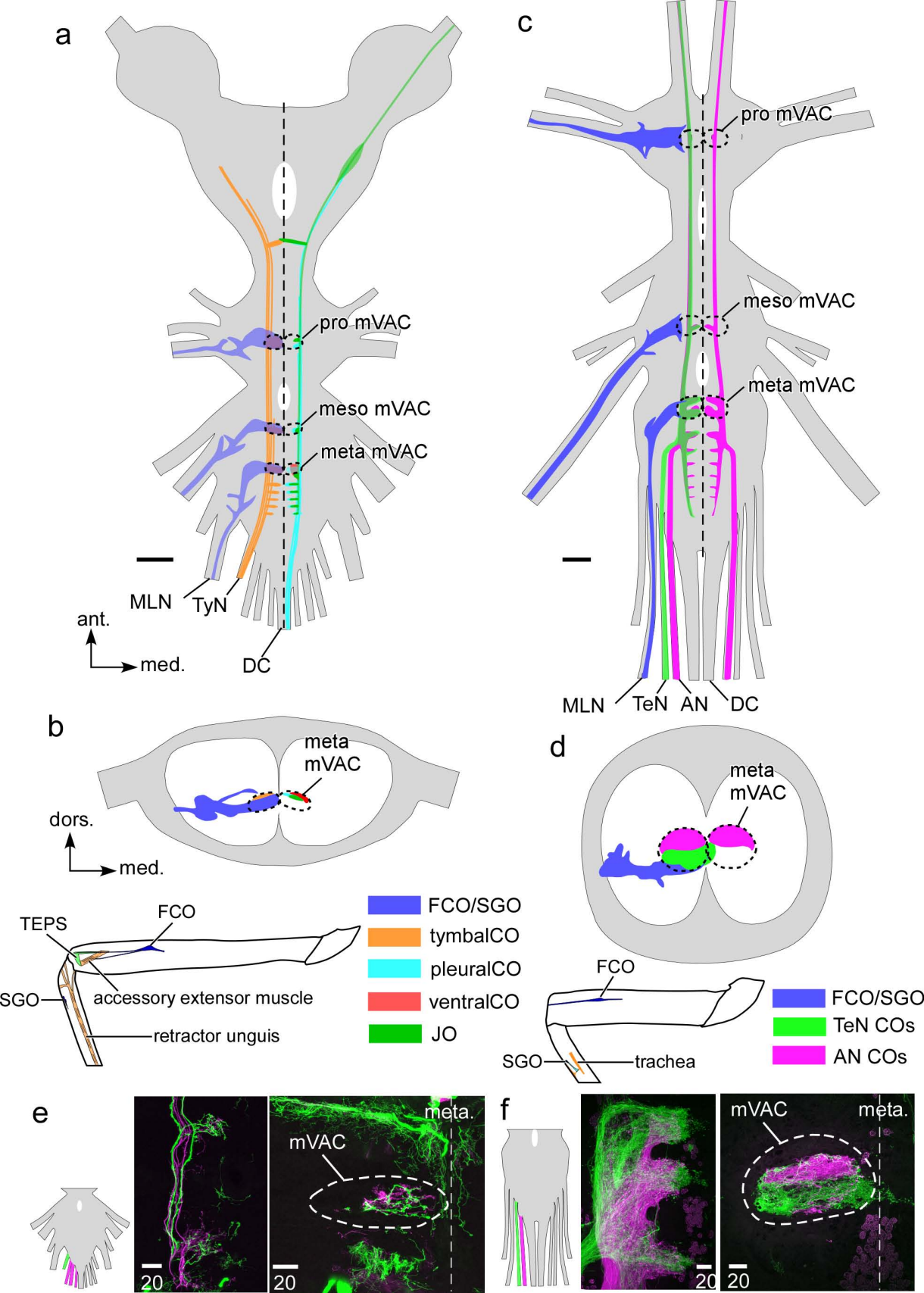
a
pro mVAC
meso mVAC
meta mVAC
MLN
TyN
DC
ant.
med.
c
pro mVAC
meso mVAC
meta mVAC
MLN
TeN
AN
DC
b
meta
mVAC
dors.
med.
TEPS
FCO
SGO
accessory extensor muscle
retractor unguis
FCO/SGO
tymbalCO
pleuralCO
ventralCO
JO
d
meta
mVAC
FCO
SGO
trachea
FCO/SGO
TeN COs
AN COs
e
meta.
mVAC
20
20
f
mVAC
meta.
20
20

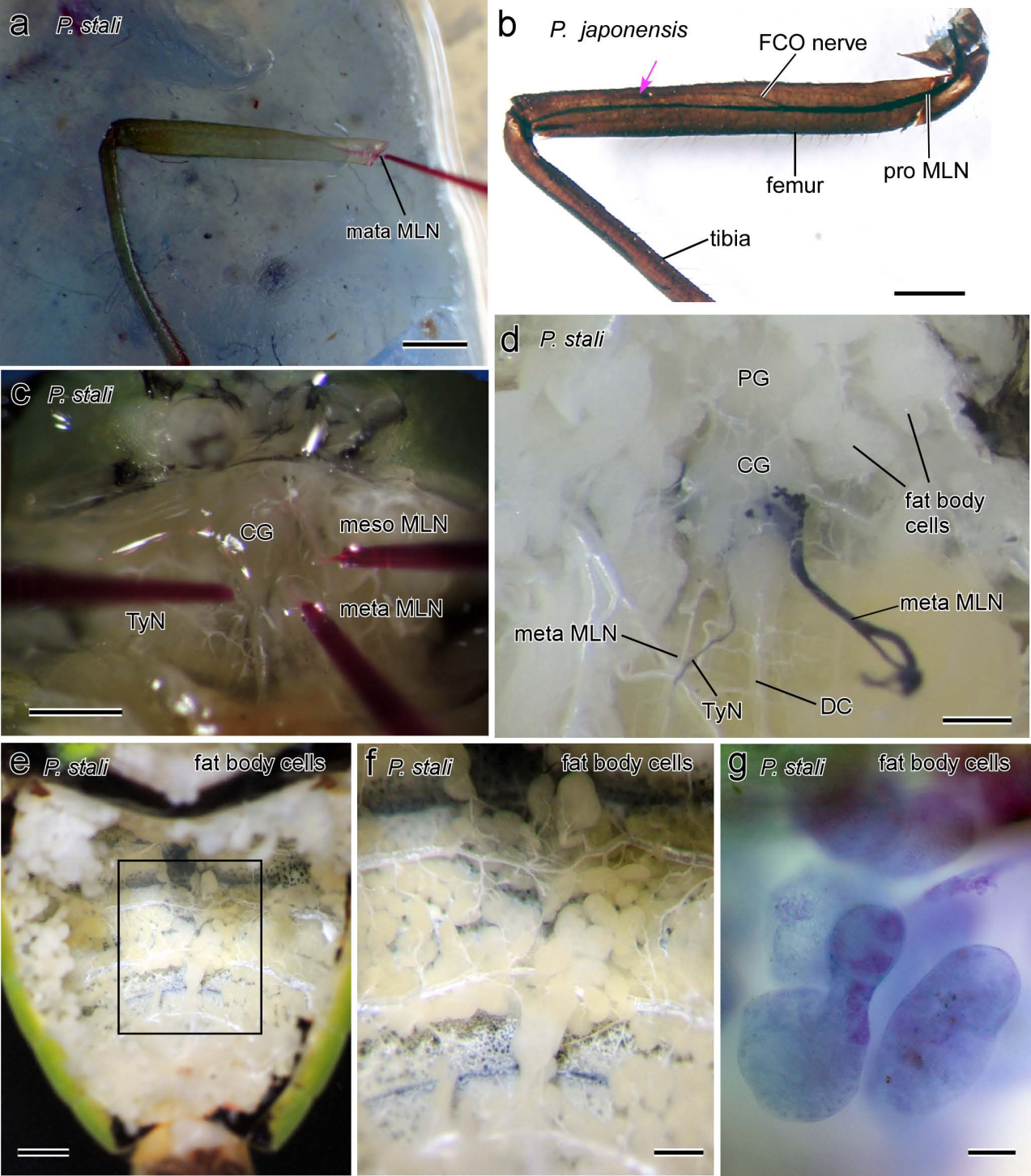
a P. stali
mata MLN
b P. japonensis
FCO nerve
femur
pro MLN
tibia
c P. stali
CG
meso MLN
TyN
meta MLN
d P. stali
PG
CG
fat body cells
meta MLN
meta MLN
TyN
DC
e P. stali
fat body cells
f P. stali
fat body cells
g P. stali
fat body cells

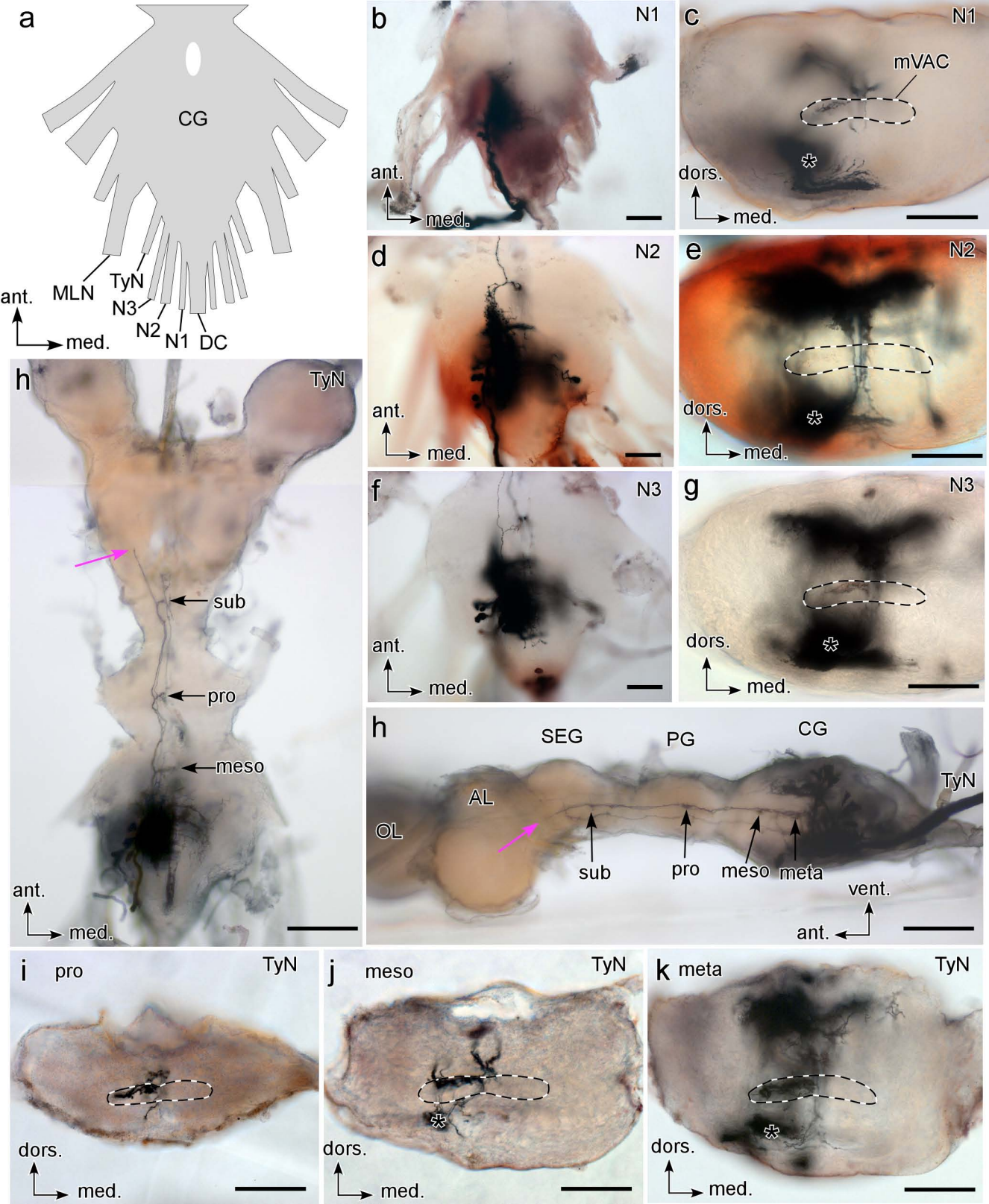
a
CG
MLN
TyN
N3
N2
N1
DC
ant.
med.
b
N1
ant.
med.
c
N1
mVAC
dors.
med.
d
N2
ant.
med.
e
N2
dors.
med.
f
N3
ant.
med.
g
N3
dors.
med.
h
TyN
sub
pro
meso
ant.
med.
h
SEG
PG
CG
TyN
AL
OL
sub
pro
meso
meta
vent.
ant.
i
pro
TyN
dors.
med.
j
meso
TyN
dors.
med.
k
meta
TyN
dors.
med.

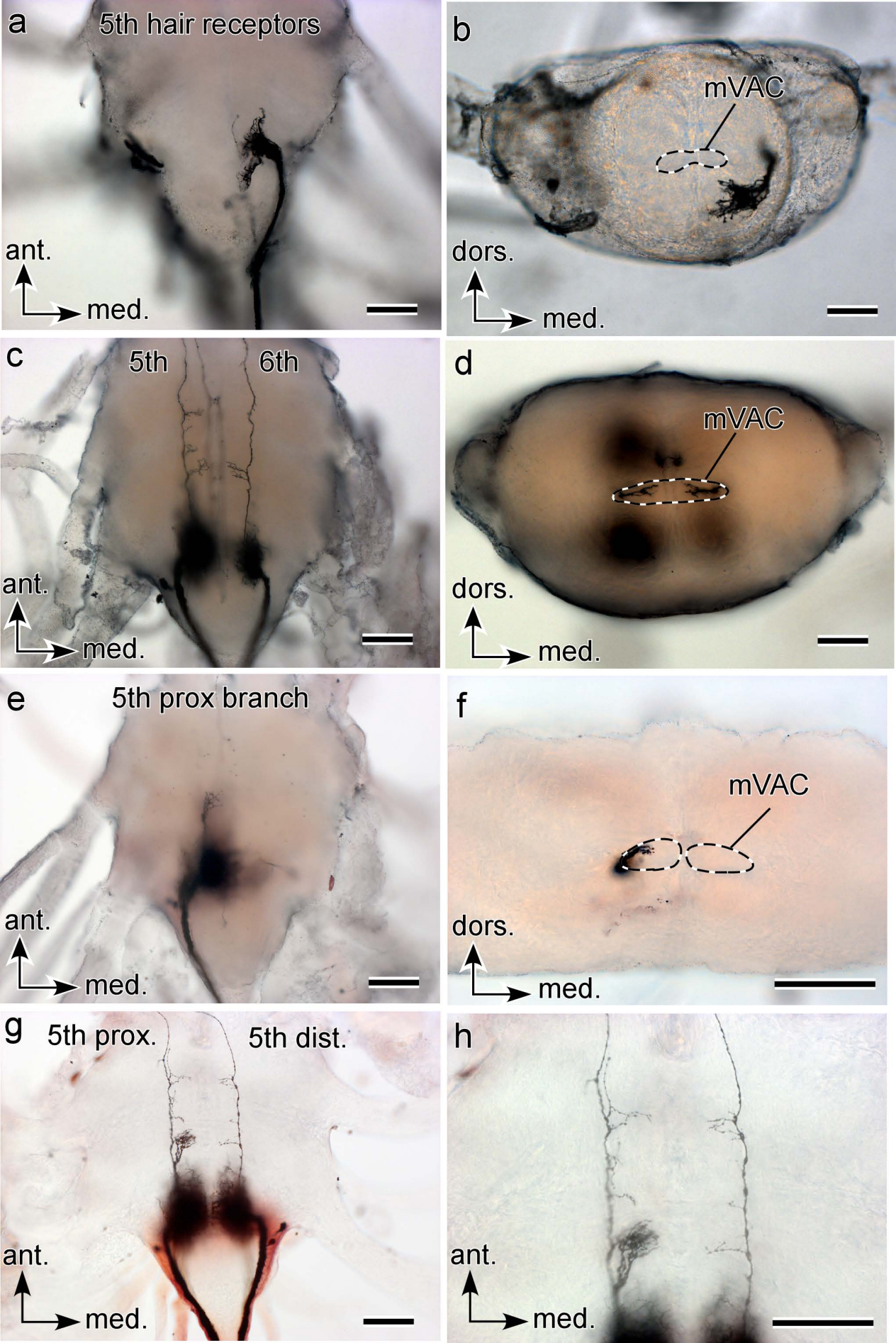
a
5th hair receptors
ant.
med.
b
mVAC
dors.
med.
c
5th
6th
ant.
med.
d
mVAC
dors.
med.
e
5th prox branch
ant.
med.
f
mVAC
dors.
med.
g
5th prox.
5th dist.
ant.
med.
h
ant.
med.